Many thanks to Anonymous Referee 1 for the contributions, and particularly for raising several pertinent questions that have helped to improve the clarity of the manuscript. The main changes include the influence of long-lasting El Niño and QBO on the results. In the following, we address all the points raised in the review (denoted by italic letters). The references to the manuscript as well as substantial changes in the manuscript are highlighted in red.

1. ***In my opinion, the current "Conclusion" section is rather a summary of the previous results. I think the paper would substantially benefit if you would also state the actual consequences of the presented results.***

   A. We did substantial changes in the "Discussion" and "Conclusions" section. The "Conclusions" section is completely reorganized, it includes both the results and brief explanation about the causes of ENSO related anomalies.

2. ***Please show some of the indicated/discussed differences in an extra panel/plot in the figures, for which the differences are relevant, e.g. Fig. 2. This would make the discussion and understanding of your line of arguments way easier.***

   A. In the revised draft, the results from the long-lasting El Niño years are included (see Figure 3, Figure 10, and Table 2). The main conclusion about the long-lasting El Niño events can be summarized as "The duration and intensity of El Niño related anomalies may be reinforced through the late summer and fall if the El Niño conditions last until the following winter".

   The influence of QBO phases on the results are shown in Figure 10 and Figure 11 in the manuscript. The text is also adjusted in the discussion section, correspondently (P21 L.11-22). The main result is that the ENSO related anomalies are enhanced (weakened) during the easterly (westerly) phase of the QBO. The details are included in the text.

   The figures below show some extra results from the long-lasting El Niño years. The SF (Figure RL 1) and VP (Figure RL 2) distributions show strongest anomalies during the long lasting El Niño years compared to all El Niño years. Figure RL 3 shows strongest Hadley circulation during long lasting El Niño years.

   Accordingly, the ozone concentrations in the tropics show weak intrusions from the subtropics during summer (Figure RL 4). This indicates that if El Niño does not decay until the following summer, the influence of El Niño on the ASM anticyclone and ozone will last longer.

3. ***In many of the analyses the differences of El Nino/La Nina decay after a couple of months and sometimes the results for El Nino seem to lag the results with respect to La Nina (e.g. Fig. 8 bottom). Please comment on how much of the observed differences is explicable through a time lag as e.g. diagnosed in the onset of the ASM anticyclone.***

   A. The draft (Figure 3) shows that the onset date of the ASM anticyclone after El Niño is about a half month later than after La Niña. We diagnose the time lag of MLS ozone after El Niño based on the same region ([5° N, 20° N; 40° E, 120° E]) as the zonal wind in Figure RL 5. Because of the difference of in-mixing and the difference in onset date of ASM anticyclone, the ozone concentrations in this domain after El Niño winters are lower than after La Niña winters. We take the onset date calculated from zonal wind (see Figure 3 in the draft)for La Niña years, the ozone concentration following El Niño winters reach the same ozone value as following La Niña winters after $\sim$ 20 days later. This can be the approximate estimate of the time lag diagnosed in the onset of the ASM anticyclone from the observation.

4. ***P.13 L.2-4: To me the differences in O3 are small in JJA in Fig.7 and the significance decreases strongly from AMJ to JJA. Further I do not see any real indication that ozone is lower after La Nina in the ASM AC in JJA. Also the statement relating this result to SF and VP is unclear (to me the differences for SF and VP are small as well). Please add plots showing the differences. This would help to follow your***

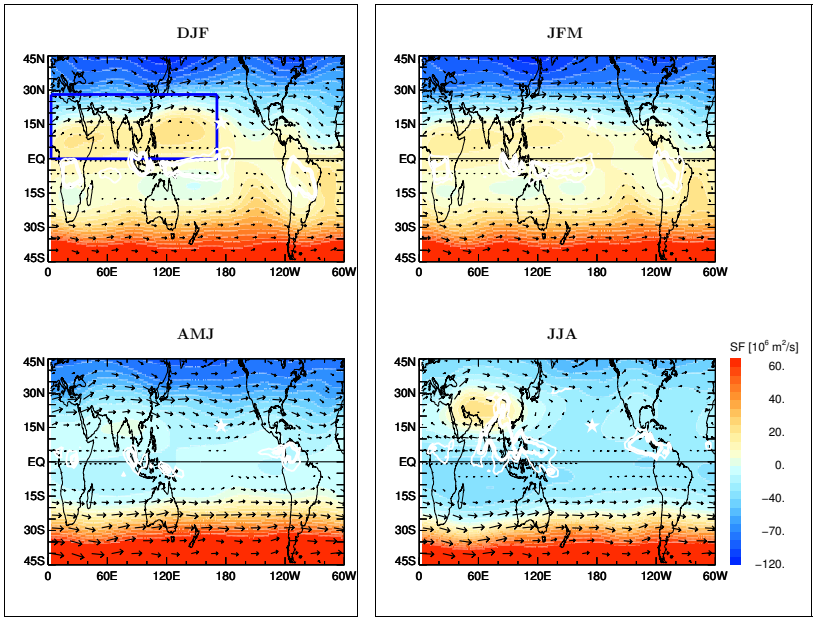

Figure RL 1: Stream function (SF, in 10^6 m^2/s) at θ=380 K for months following long lasting El Niño (1987 and 1992) winter until summer (from top to bottom). The arrows represent the rotational horizontal wind. White isolines indicate the strong convection regions based on OLR (thick and thin lines represent 210 and 220 W/m^2 contours) data, respectively.

statements. You even state yourself that the differences are small: P7 L.6-9....Please clarify and comment on this.

A. You are right, the significance indeed decreases strongly. We emphasized the decrease of the significance before. We agree with your point, so we changed it as "During the mature phase of the ASM anticyclone (JJA), the number of black dots decreases strongly, but there is still a region of significant in-mixing differences on the ozone tongue as well as the extratropical side of the tropopause." in the text (P.12 L.31-32) now. The MLS ozone in JJA (Figure 7, bottom) shows that the region of ASM anticyclone after La Niña events is larger than after El Niño, and the ozone in this region after La Niña events is lower than after El Niño events. The difference between La Niña and El Niño composites is small for SF and ozone distribution in JJA. Our results show that the difference can last from DJF to MJJ, but it's not significant in JJA. We removed VP-related arguments from the manuscript because the ozone distribution is more affected by the SF patterns.

5. ***P.7 L.6-9: You state that the forcing of the summer dynamics is only weakly related to the winter forcing. However, there is a well-known connection of ENSO and the Indian summer monsoon. You also include a reference (Chowdary et al 2016)regarding this issue. Further, have you checked how the summertime results change if the composites are not made using ENSO prior to the monsoon season but ENSO subsequent to the monsoon, i.e. assessing the influence of developing El Nino/La Nina events on the ASM? Assessing these differences could really improve the understanding of the connection between ENSO and the ISM. Also the ENSO phase during NH summer might influence your results, i.e. your results might depend on if the ENSO phase is transitioning from El Nino to La Nina or vice versa or if you have a no-decay El Nino (this example is even mentioned in the discussion) or no-decay La Nina.***

   A. From Figure 7 (JJA, bottom), we can see that the influence from ENSO is significantly decreased from the large scale perspective, but the difference (the dots in the figure) still exists from the small scall perspective (such as India, strong in-mixing region). We didn't investigate the results based on different ENSO

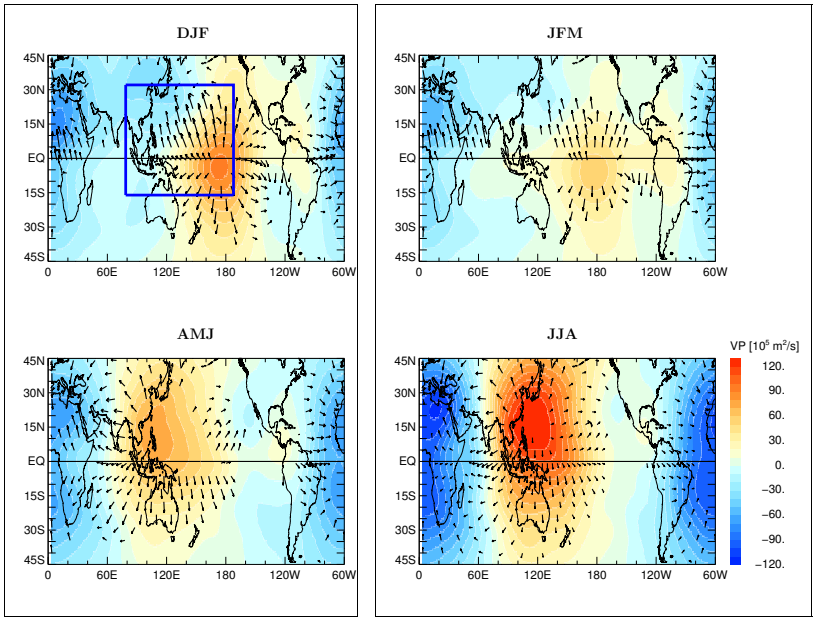

Figure RL 2: Same as Figure RL 1 but for the velocity potential VP (in 10^5 m^2/s) at θ=380 K with arrows denoting the divergent part of the horizontal wind.

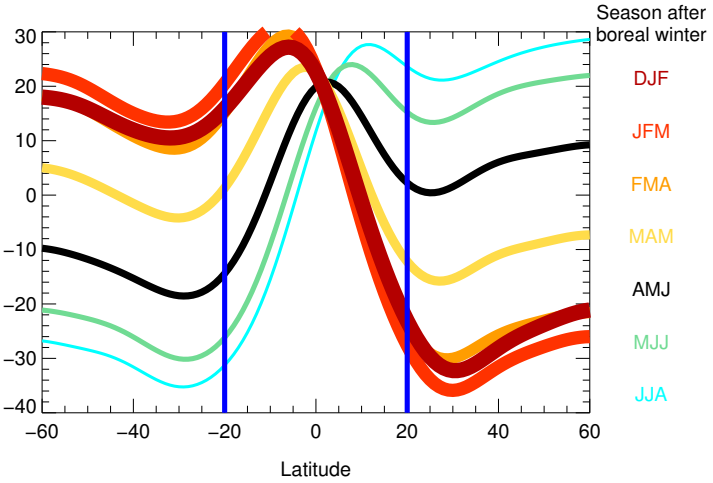

Figure RL 3: Zonal mean of the velocity potential at θ=360 K defining the Hadley circulation and calculated for long lasting El Niño years (1987 and 1992). The average intensity of Hadley circulation calculated for the domain of [20° S, 20° N] (bottom).

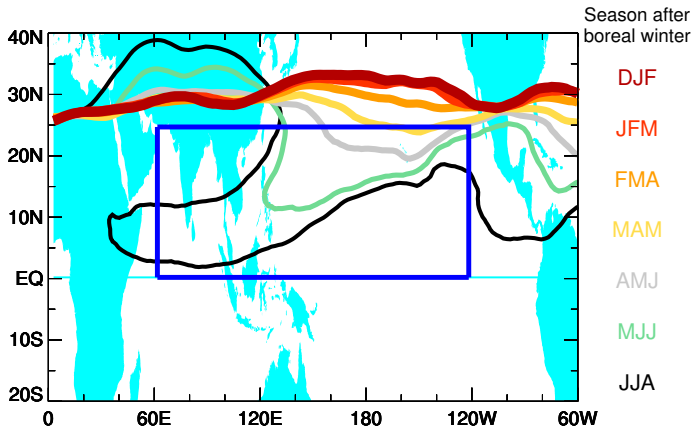

Figure RL 4: Isolines of CLaMS ozone (120 ppbv at θ=380 K for different seasons following long lasting El Niño (b) winters (from DJF (red) to JJA (grey)).

phase because we don't have sufficiently long period sample as in the paper from Chowdary et al. 2016 (1876-2007). This is why we put the influence of long-lasting El Niñoevents in the discussion, not in a new section.

6. ***P.18 L.24: "The change..." This paragraph is difficult to follow. Please rephrase to make your analysis easier to follow. Also I do not understand why you are excluding in particular the ENSO events 1997/1998 and 2006/2007. Is this simply made to have a remaining set which contains an equal amount of El Nino years in QBO east and west phase? If so, I do not see why you would exclude these two events and not some others and I do not come to the conclusion that the results are robust because of this analysis. A better way might be to split the El Nino/La Nina events completely between QBO east and west and than make a comparison. (I know that this leads to a very limited number of cases, especially for the La Nina events. But you do this anyhow when you look at the no-decay El Ninos). The number of considered ENSO events could be increased by including/checking, JRA-55, which extends back to 1958.***

   A. We agree with your suggested method to investigate the influence of QBO phase. Figure 10 and Figure 11 in the draft show the results during westerly and easterly phase. We also change the statement in the text (for details, see the "Discussion" section). The main change can be summarized like "The results at 380 K from CLaMS simulations show that ozone concentration after La Niña events is higher than after El Niño events during both phases of QBO, but the difference between the two composites during easterly phase is lager than during westerly phase. The SHADOZ ozone data shows that the ozone concentration after La Niña events is higher (lower) than after El Niño events in the UTLS (middle troposphere) during both phases of QBO, while the two composites during easterly phase also show larger difference comparing to westerly phase. This indicates that our results about the ENSO effects are robust, but the difference will be enhanced (weakened) during easterly (westerly) phase".

7. ***P.11 L.2: You assess the significance of the changes of the Hadley circulation using a mean of VP from 20S to 20N. As a sensitivity: How does this change if you use a region centered around latitude of the peak value of \overbar{VP}, or a mean over a region where overbarVP falls below a certain threshold?***

   A. We checked the significance of the changes of the Hadley circulation using a mean of VP in the domain of [5° S, 5° N], [10° S, 10° N], [15° S, 15° N], [20° S, 20° N], [25° S, 25° N] and [30° S, 30° N]. The results show that the significant difference can last from DJF to FMA in the domain of [5° S, 5° N], [10° S, 10° N] and [15° S, 15° N], and the significant difference can last from DJF to MAM in the domain of [20° S, 20° N],

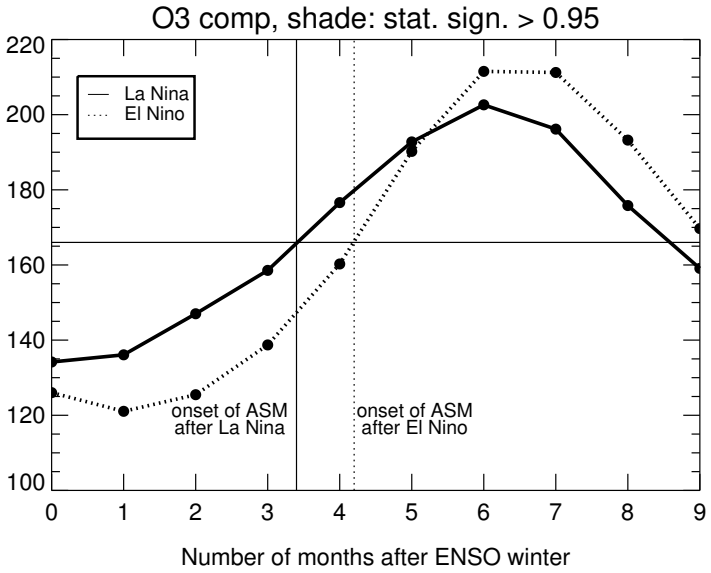

Figure RL 5: Mean ozone in the tropics over south-east Asia ([5° N, 20° N; 40° E, 120° E]) following La Niña and El Niño winters at 380 K. The zero mark in x-axis denotes the middle of the DJF season (i.e., 15 January).

[25° S, 25° N] and [30° S, 30° N]. We choose the domain of [20° S, 20° N] because it includes all the peak locations from DJF to JJA.

8. ***P.2 L.31-33: This sentence is strange; the part "... like weather patterns or precipitation..." seems disconnected from the previous part of the sentence.***

   A. It's changed as "This is in contrast with a large number of investigations connecting ENSO with the tropospheric variability of the ASM, such as weather patterns and precipitation, which have a long tradition starting with the pioneering studies of Walker (1923) and Bjerknes (1969)." in the manuscript (P.2 L.33-35).

9. ***P.3 Fig. 1: You might want to add a reference to Konopka et al. 2016; same for Table 1.***

   A. The data from Figure 1 and Table 1. is extended from the period 1979-2013 to period 1979-2015. We also include "As in Konopka et al. (2016)" in the text for Figure 1 and Table 1.

10. ***P.3 L.3: Add that you are using also O3 data from a Lagrangian CTM.***

    A. "Lagrangian model ozone data" is included in the text (P.3 L.5).

11. ***P.4 L.4: Please add a reference for the Monte Carlo method you are using and add a short explanation what the Monte Carlo method does.***

    A. The reference and short explanation are included in the text (P.4 L.10-12) like "Monte Carlo significance test procedures consist of the comparison of the observed data with random samples generated in accordance with the hypothesis being tested (Hope, 1968)".

12. ***P.4 L.6: You are using data for 2016 also as December 2015 is listed as El Nino month....so for the assessment of changes related to ENSO you are also using MLS, ERA-I and CLaMS data for 2016, right? Please update this in multiple occasion throughout the paper.***

    A. The data from 2016 is not included in our research. We use the data until the winter of 2015.

13. ***P.5 L.4-6: Add the information of how many El Nino (La Nina) events are considered to the information of how many months contribute to the composites. IS the information on how many months are considered even important, as you show DJF composites anyhow? Do you average the months or the years when averaging the data over multiple years? Please clarify!***

    A. The information of how many El Nino (La Nina) events is included in the text like "MLS measurements provide 8/6 months of data for the 3/3 La Niña/El Niño episodes from 2004 to 2015. Respectively there are 14/11 months of data for the 5/5 La Niña/El Niño events from SHADOZ ozondesondes covering the period 1998-2015". Because ENSO doesn't always show strong signal in the whole DJF, we also include the months in our draft. We average the months when averaging the data over multiple years.

14. ***P.5 L.4: Please stick with one way: "6/8 ... La Nina/El Nino" or "6 (8) ... La Nina (El Nino)" throughout the whole paper.***

    A. The expression is changed throughout the paper (P.5 L13-15). It's like "MLS measurements provide 8/6 months of data for the 3/3 La Niña/El Niño episodes from 2004 to 2015. Respectively there are 14/11 months of data for the 5/5 La Niña/El Niño events from SHADOZ ozondesondes covering the period 1998-2015".

15. ***P.5 L.9: Correct the URL for OLR data from NOAA and add statement to the acknowledgment! Probably also for the ENSO data!***

    A. The URL for OLR is corrected in the test with "https://www.esrl.noaa.gov/psd/data/gridded/data.interp_OLR.h (P.5 L19). The statement is included in the acknowledgment like "OLR data is provided by NOAA.".

16. ***P.5 L.24: "The climatological..." add "with respect to La Nina and El Nino conditions" or something like that and finish with "building the analogue composites for OLR as for the SF" or something similar.***

    A. The expression is changed as "The climatological sources of heat can be approximated by the lowest values of the OLR. The analogous composites for OLR (magenta contours in Figure 2) as for the SF are built with respect to La Niña and El Niño conditions" in the text (P.7 L3-4).

17. ***P.5 L.26: Should this better state: "anticyclones are mainly located over the maritime continent during La Nina ... partially shifted towards the western Pacific during El Nino events.". Please clarify this sentence.***

    A. Here we use the OLR data to indicate the heating source of the anticyclone. So this statement is about the different locations of the heating source during La Niña and El Niño years not the locations of anticyclone.

18. ***P.7 Fig.3: What does the hatching indicate in this figure? Remove if unnecessary.***

    A. The hatching was supposed to help to know the onset date of the ASM and recognize the onset date difference between El Nina and La Nina. Probably it's confusing, so the hatching is removed now.

19. ***P.7 L.10: Please add "climatological" after "mean" and add that the climatological mean is not shown. Otherwise it is hard to understand what you are referring to.***

    A. The "climatological" is added in the text (P.8 L1). Here, the mean climatological anticyclone in AMJ means the climatological after El Nino and La Nina events, which is showed in the figure.

20. ***P.8 Fig. 4: Consider to make the hatching a little darker (for printed versions of the paper). Also in similar plots (e.g. Fig. 6).***

    A. The hatching is changed to grey shading for Figure 4, Figure 6, Figure 8 and Figure 10.

21. ***P.8 L.17: Change to "The domain is supposed to...". How do the results change if you would check for the size of the area which lies within a specific VP contour, instead of using a fixed rectangle, where you might end up averaging positive and negative values of VP?***

    A. The text (P.10 L14-16) is changed as "The blue rectangle in Fig. 5, defined as [30° S, 40° N; 90° E, 140° W], represents the region of the ascending branch of the Walker circulation. The mean positive values over this blue rectangle are calculated. The domain allows quantification of the average upwelling of the Walker circulation". Here, we just average the positive values in the domain to get the intensity of upwelling. We clarify this in the text now. The statistical results don't change if we change the size of the area.

22. ***P.9 Fig.5: You may want to add a description for the blue rectangles and keep them in all panels, to guide the eye. P.10 Fig.6: The different colours of the seasons are difficult to read, especially JJA MJJ and MAM. Also consider to add a plot showing the differences.***

    A. The description is included in the text (P.10 L14-16) like "The blue rectangle in Fig. 5, defined as [30° S, 40° N; 90° E, 140° W], represents the region of the ascending branch of the Walker circulation. The mean positive values over this blue rectangle are calculated. The domain allows quantification of the average upwelling of the Walker circulation". The blue rectangles are added for all panels. The colours in Figure 6 are changed, and the plot about the difference is included in Figure 6 (c).

23. ***P.11 L.32: "Ozone in mixing...." I do not see why they are delayed. Please refer to the figures showing this time delay.***

    A. Comparing to SF, which the largest difference occurs in DJF, the largest difference of ozone in mixing occurs in AMJ. The text is changed correspondingly (P.12 L28).

24. ***P.12 Fig.7: Do you show ozone isolines at 380K or at the tropopause altitude for the black contours? This is also confusing in other figure captions and multiple occasions in the text (e.g. P.13 L.6, P.14 L.9, ...). If it is at 380K simply state "at 380K". Please clarify!***

    A. The colorbar shows the ozone distribution at 380 K, but the ozone isolines represent the tropopause altitude. The description is slightly changed in the text as well.

25. ***P.14 L.2: I do not think that "Thus" is the right wording here.***

    A. The description is changed in the text (P.12 L30).

26. ***P.15 L.10: How do CLaMS results and MLS measurements compare if you restrict the CLaMS data to the period 2005-2015?***

    A. The ozone concentration after El Niño is about 11 ppbv lower than after La Niña if we restrict the CLaMS data to the period 2005-2015, which is similar to the results (12 ppbv) from the period 1979-2015.

27. ***P.17 Fig.11: I guess you are showing longitudinal averages in the west and central Pacific region of zonal anomalies. Please try to be clear (also in several parts of the text). Also add "the" in front of "..../theta = 380K...".***

    A. Yes, we are showing the longitudinal averages in the west and central Pacific region of zonal anomalies. See the new caption in P.20 Figure 12.

28. ***P.18 L.13: Change "three years" to either "two years" (1987 and 1992) or "two ENSO events" or something similar.***

    A. The long lasting El Nino year 1982 is also included, so the text is changed as "three years" (P.21 L3).

29. ***P.18.L14: "In particular...". Please add the time periods when the ASM (Hadley circu- lation) is weaker (stronger). This will also help to follow your conclusion in the following sentences, which is not clear at the moment.***

    A. The time period is included and results are changed in the text (see P.21 L.3-10).

30. ***P.2 L.18: Add the full version of STE.***

    A. The full version of STE (stratosphere-troposphere exchange) is included in the text (see P.2 L.16).

31. ***P.3 L.8: Add full version of abbreviation NOAA = National ....***

    A. The full version of NOAA (National Oceanic and Atmospheric Administration) is included in the text (see P.3 L.10).

32. ***P.5 L.1: Maybe change to: "Ozone distributions are used to validate our diagnostics of the flow and to understand the effect....in the UTLS region."***

    A. It's changed in the text (see P.5 L.10).

33. ***P.5 L.16: Change to: "The panels in Fig. 2 start from ..."***

    A. It's changed in the text (see P.5 L.26).

34. ***P.5. L.3: Remove ")(" and add "," after "(SHADOZ...".***

    A. It's changed in the text (see P.5 L.12).

35. ***P.5 L.30: add "during NH summer" or "during JJA" after "(ASM) anticyclone"***

    A. "during NH summer" is included after "(ASM) anticyclone" (see P.7 L.9-10).

36. ***P.5. L.32: I guess that "asymmetric" should be changed to "antisymmetric".***

    A. It's changed as anti-symmetric in the text (see P.7 L.11).

37. ***P.7 L.6 : "stronger localized" do you mean "stronger and more localized" or simply "more localized"?***

    A. It's changed as "stronger and more localized" in the text (see P.7 L.17-18).

38. ***P.8 L.12: I guess you want to state: "In spring (FMA)" the differences between the two composites are smaller than in winter."***

    A. Yes, the text is changed (see P.10 L.9).

39. ***P.9 L.9: Add blank after "variability"***

    A. The blank is added in the text (see P.3 L.11).

40. ***P.10 L.4: Please add ($\overline{VP}$), to indicate that this is the zonal mean of VP.***

    A. $\overline{VP}$ is added in the text (see P.10 L.20).

41. ***P.10 L.8: Add "winters"/"events" or "episodes" after El Nino and change "with decreasing ENSO differences" to "and the differences between the El Nino and La Nina composites decrease from DJF to JJA"***

    A. It's changed as "This circulation is weaker after La Niña than after El Niño episodes, and the differences between the La Niña and El Niño composites decrease in summer" in he text (see P.10 L.23-24).

42. ***P.14 L.8: I guess on should used "as" instead of "like"; this also occurs at multiple occasions in the text (e.g. P.5 L.8). Also add "(top)" after "Fig. 8".***

    A. “like” is replaced as “as” in all the occasions in the text text (e.g. P.16 L.14).

43. ***P.15 L.21: If the sentence starts with Figure you should write "Figure" instead of "Fig." (this is easier to read and as I know this is Copernicus standard, check for other parts in the text)***

    A. The “Fig.” is replaced as “Figure” if it’s at the beginning of the sentence in the whole paper.

44. ***P.15 L.12: Change "... simulations above ..." to "... simulations as described above ..."***

    A. It’s changed in the text (see P.16 L.31).

Many thanks to Anonymous Referee 3 for thoughtful comments and suggestions that have helped to improve the presentation and completeness in this manuscript. The comments from the referee are denoted by italic letters. Our responses and a brief summary of related changes to the manuscript are given below. The references to the manuscript, in particular substantial changes in the manuscript are highlighted in red.

1. ***The colorbars have been improved for most plots since I reviewed the paper last. I think the red/blue colorbar could also be used for Figure 11, I'm not sure why that one is different.***

   A. The colorbar is changed for Figure 12 (Figure 11 in the ACPD version).

2. ***Page 3, line 1-2: It's unclear to me what is meant by "We investigate how long ENSO related statistically relevant differences can be diagnosed". What is meant by long? You investigate the length of these relationships? Or is it meant to mean you look at differences over a long time period? It's not clear.***

   A. Typically, ENSO occurs in winter, but the influence of ENSO does not just exist in winter. We investigate the time period of ENSO influence. In the text (P.5 L.1), it's changed as " we investigate how the ENSO winter signal propagates into the following seasons".

3. ***Page 3, lines 14-15. Why this particular threshold of 0.9? What is the sensitivity to threshold? (i.e., how much do the results change for different thresholds?)***

   A. Usually, the threshhold should be 1. We use the threshold of 0.9 to get larger sample. The results don't change too much if we change it as 1 (see also Konopka et al., 2016). Below we show the differences in SF using the threshold with 1. Figure RL 1 and Figure RL 2 show the strength of the anticyclone might be slightly different with the results in the manuscript if we take 1 as the threshold. However, the meridional disruption during El Niño are weaker compared to La Niña winters, the anticyclone after La Niña events is stronger than after El Niño, and the differences between La Niña and El Niño composites persist from winter to early summer. These are the same conclusions as in the draft, so our results in the manuscript are robust.

4. ***Page 4, lines 3-4: Might explain more is the significance assessed using a 2-tailed student t-test, for example?***

   A. Figure RL 3 shows the statistical difference results (black dots) between El Nio and La Nia composites from the 2-tailed student t-test from MLS ozone at 380 K. The significantly different regions from the 2-tailed student t-test are less than the regions from the Monte Carlo (Figure 7 in the draft) significance test. But the results here also show significant difference in the regions of strong in-mixing. During the mature phase of the ASM anticyclone (JJA), the number of black dots decreases strongly like in the Monte Carlo significance test. So the statistical difference results from the Monte Carlo significance test are robust.

5. ***Page 7, lines 2-5: Do you have a sense for how robust these ENSO features are relative to internal variability? The reanalysis period is still relatively short to evaluate dynamical differences. See, e.g., Deser et al. (2017).***

   A. We agree that the reanalysis period is short. We don't really know how robust the ENSO features are relative to the internal variability. This needs further investigation, but is beyond the scope of this study. We plan to use CLaMS-climate coupling model in the future. So we will return to this point in the further work.

6. ***Figure 3/4/6- indicate in caption what the different colored dots mean, if anything. Figure 3 should also have something about the dashed region being significant (it's a bit confusing because in Fig. 4 the dashed region indicates significance, however, in Figure 3 the differences should be insignificant by JJA, correct?). Finally, in Fig 3 the x-axis is labeled as "Month" but Figure 4 says "Month after***

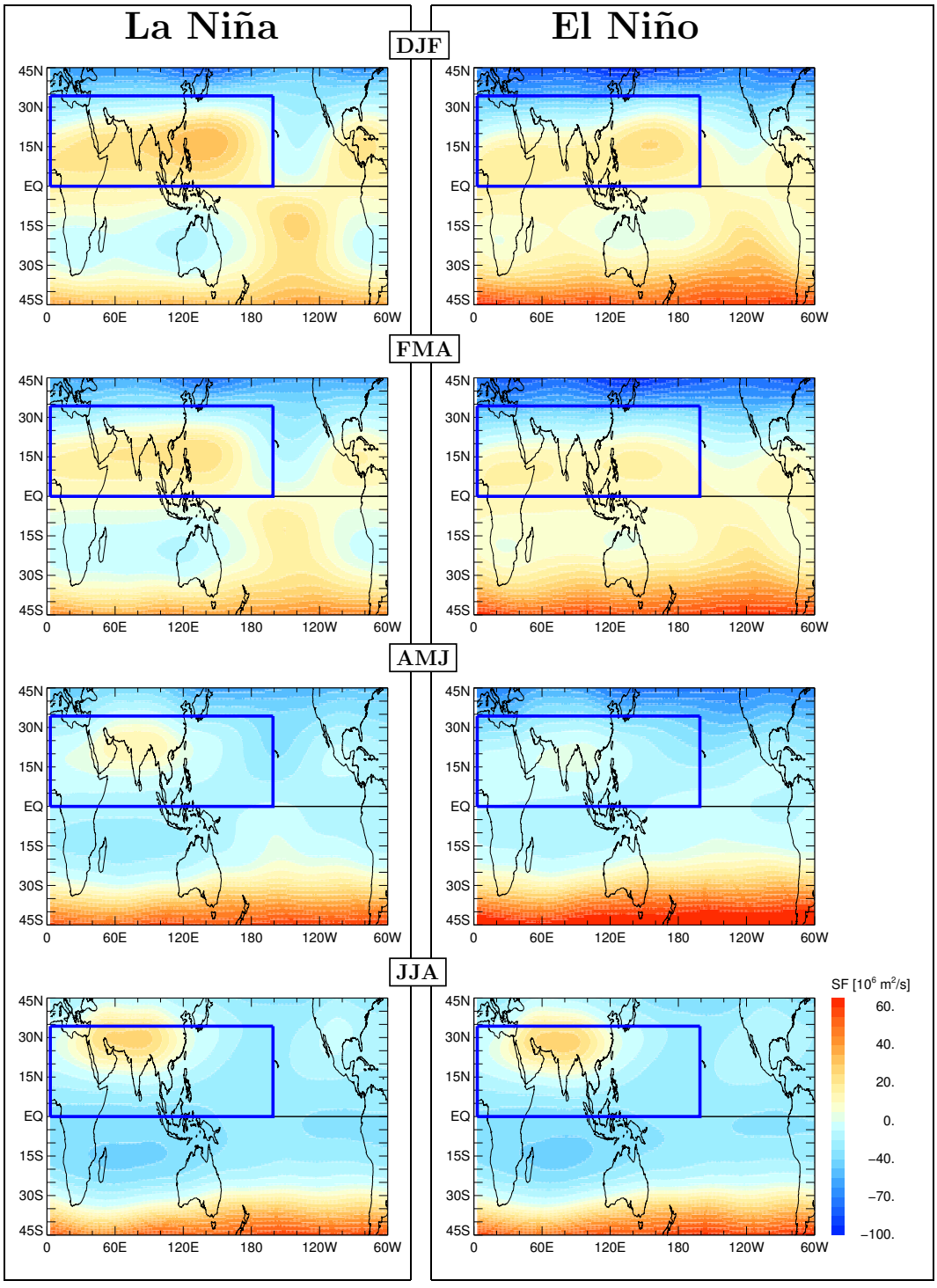

Figure RL 1: Climatologies (composites) of the stream function (SF, in 10^6 m^2/s) at θ=380 K calculated from ERA-Interim (1979-2015) for months following La Niña (left) and El Niño (right) winters until summer (from top to bottom). The blue rectangles mark the locations of strong anticyclone in NH.

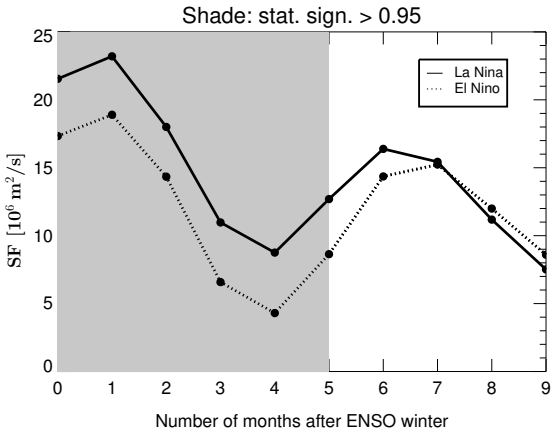

Figure RL 2: The average value of the stream function in the domain of [0° N, 35° N; 0° E, 160° W] for La Niña (solid line) and El Niño (dotted line) composites at θ=380 K. The grey shading region denotes the period with statistically significant differences between the two composites.

DJF". Month makes more sense to me if these are indeed the months; does "Month after DJF" imply that 0=March?? Or does 0=JFM? It would help to label the axis tick marks with exactly what is meant.

A. The colored dots in Figure 3/4/6 meant different month or season. We changed all of them to black color in revised paper because the x-axis includes the time information. The dashed lines in Figure 3 were supposed to help to recognize the onset date difference between El Nina and La Nina. Probably it's confusing, so the hatching is removed now. The climatology of U wind is calculated from monthly composite, so the x-axis label marks the month information in Figure 3. The x-axis label represents the season information in Figure 4/6 because the climatologies are calculated from the seasonal composites. To make the figures easy to understand, we changed the x-axis labels and captions in Figure 4/6.

7. ***Page 2, line 30: "only few"->"few" or "only a few"***

   A. It's changed in the text (P.2 L.32).

8. ***Page 5, Line 26: should be "mainly in the western Pacific"***

   A. It's changed in the text (P.7 L.5-6).

9. ***Page 8, Line 3: "is by a factor" -> "is a factor"***

   A. It's changed in the text (P.8 L.17).

10. ***Page 10, Line 4: "are by more than three times" ->"are more than three times"***

    A. It's changed in the text (P.10 L.21).

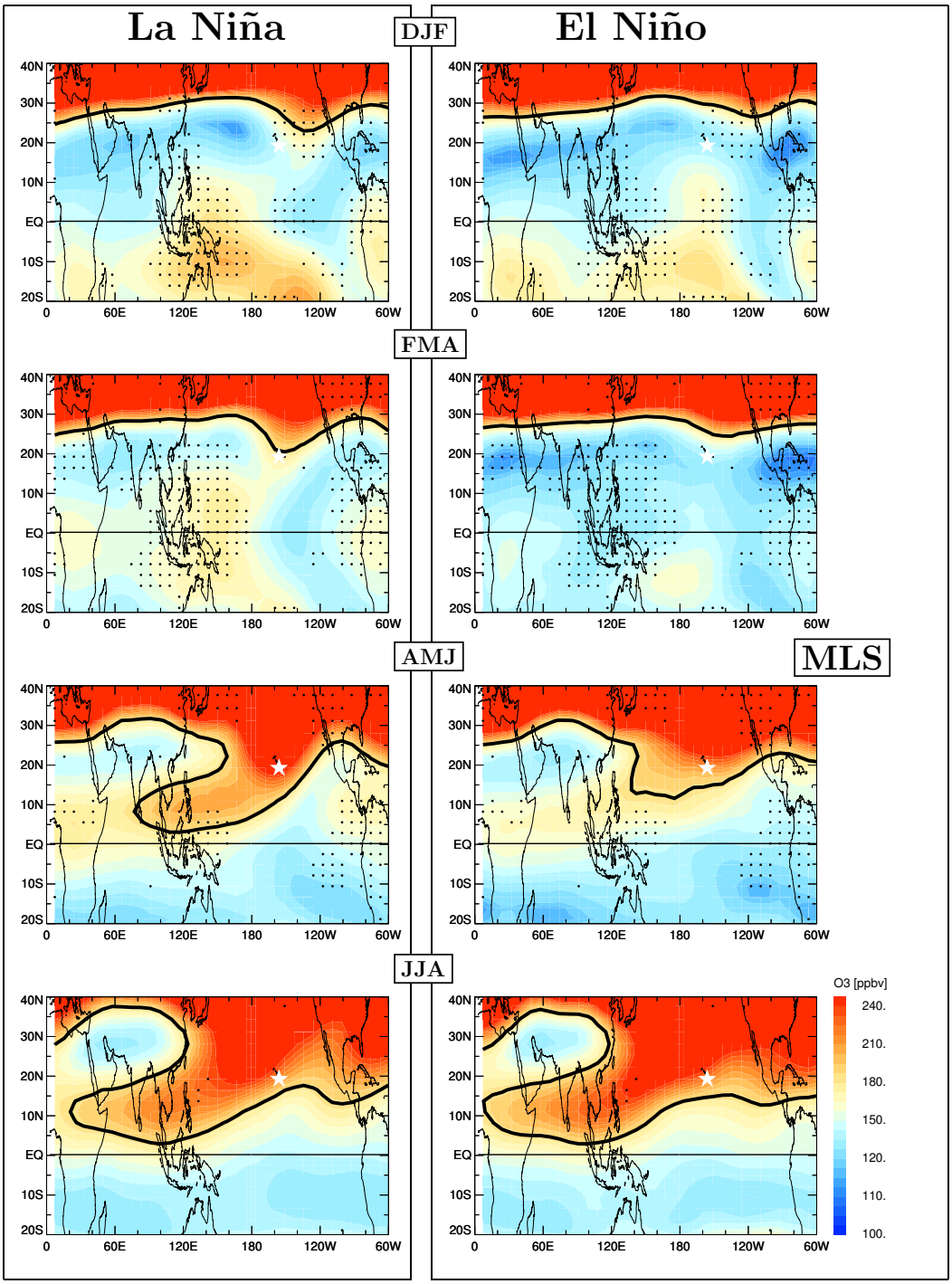

Figure RL 3: Seasonal ozone climatology derived from MLS observations (2004-2015, version 4.2) at θ=380 K for La Niña and El Niño composites from winter to summer months (from top to bottom). Regions with statistically significant differences are marked by the black dots. The black isolines represent ozone with 185 ppbv, which mark the tropopause.

El Niño Southern Oscillation influence on the Asian summer monsoon anticyclone

Xiaolu Yan[1,2], Paul Konopka[1], Felix Ploeger[1], Mengchu Tao[1], Rolf Müller[1], Michelle L. Santee[3], Jianchun Bian[2,4], and Martin Riese[1]

[1]Forschungszentrum Jülich (IEK-7: Stratosphere), Jülich, Germany
[2]Key Laboratory of Middle Atmosphere and Global Environment Observation (LAGEO), Institute of Atmospheric Physics, Chinese Academy of Sciences, Beijing, China
[3]Jet Propulsion Laboratory, California Institute of Technology, Pasadena, CA, USA
[4]College of Earth Science, University of Chinese Academy of Sciences, Beijing, China

Correspondence to: Xiaolu Yan (x.yan@fz-juelich.de)

Abstract. We analyze the influence of the El Niño Southern Oscillation (ENSO) on the atmospheric circulation and the mean ozone distribution in the tropical and sub-tropical UTLS region. In particular, we focus on the impact of ENSO on the onset of the Asian summer monsoon (ASM) anticyclone. Using the Multivariate ENSO Index (MEI), we define climatologies (composites) of atmospheric circulation and composition in the months following El Niño and La Niña (boreal) winters and investigate how ENSO-related flow anomalies propagate into spring and summer. To quantify differences in the divergent and non-divergent part of the flow, the velocity potential (VP) and the stream function (SF), respectively, are calculated from the ERA-Interim reanalysis ~~around~~ in the vicinity of the tropical tropopause ~~(~~at potential temperature level θ=380 K~~)~~. While VP quantifies the well-known ENSO anomalies of the Walker circulation, SF can be used to study the impact of ENSO on the formation of the ASM anticyclone, which turns out to be slightly weaker after El Niño than after La Niña winters. In addition, stratospheric intrusions around the eastern flank of the anticyclone into the Tropical Tropopause Layer (TTL) are weaker in the months after strong El Niño events due to more zonally symmetric subtropical jets than after La Niña winters. By using satellite (MLS) ~~,~~and in-situ (SHADOZ) observations and model simulations (CLaMS) of ozone, we discuss ENSO-induced differences around the tropical tropopause. Ozone composites show more zonally symmetric features with less in-mixed ozone from the stratosphere into the TTL during and after strong El Niño events and even during the formation of the ASM anticyclone. ~~The difference between~~ Such isentropic anomalies are overlaid with the well-known anomalies of the faster/slower Hadley and Brewer Dobson circulation after El Niño~~and~~ /La Niña ~~composites becomes statistically insignificant in late summer~~ winter, respectively. The duration and intensity of El Niño related anomalies may be reinforced through the late summer and fall if the El Niño conditions last until the following winter.

1 Introduction

El Niño and La Niña are opposite phases of the El Niño Southern Oscillation (ENSO) which ~~originates~~ originate from the coupled interaction between the tropical Pacific and the overlying atmosphere ~~(e.g., Bjerknes, 1929; Wang and Picaut, 2004)~~(e.g., Bjerknes, 19

ENSO is widely recognized as a dominant mode of the Earth's climate variability (McPhaden et al., 2006). In the troposphere, ENSO manifests in the anomalies of the zonal distribution of convection which are triggered by a positive (El Niño) and negative (La Niña) sea surface temperature (SST) anomaly in the central and eastern Pacific (Philander et al., 1989). The SST anomalies typically peak during the Northern Hemisphere (NH) winter time (hereafter, seasons refer to the NH), but prolonged events may last for months or years (Moron and Gouirand, 2003; McPhaden, 2015).

Strong El Niño events disrupt the Walker circulation and lead to its breakdown during the warm ocean phases (Wang et al., 2002). Strong El Niño events also propagate upwards above the tropopause by accelerating the Brewer Dobson ~~circulation (BDC)~~ (BD) circulation and moistening the stratosphere (Scaife et al., 2003; Randel et al., 2009; Calvo et al., 2010). Using satellite observations and model simulations of water vapour and mean age of air, Konopka et al. (2016) have recently shown that wet (dry) and young (old) tape-recorder anomalies propagate upwards in the tropical lower stratosphere in the months following El Niño (La Niña). They found that these anomalies are around $+0.3$ (-0.2) ppmv and -4 ($+4$) months for water vapour and age of air, respectively.

The Asian summer monsoon (ASM) anticyclone is a dominant feature of the circulation in the upper troposphere lower stratosphere (UTLS) during summer (Dethof et al., 1999; Randel and Park, 2006; Park et al., 2007). This nearly stationary anticyclone extends well into the lower stratosphere up to about 18 km (or $\theta = 420$ K) and effectively isolates the air masses of tropospheric origin inside from the much older, mainly stratospheric air outside this anticyclone (Park et al., 2008; Ploeger et al., 2015). This anticyclone has been repeatedly identified as a key pathway for stratosphere-troposphere exchange (STE) in summer and fall, both quasi-isentropically into the lowermost stratosphere and into the upper branch of the ~~Brewer Dobson~~ BD circulation, especially for water vapour and pollutants entering the global stratosphere (Bannister et al., 2004; Fueglistaler et al., 2005; Fu et al., 2006; Randel et al., 2010; Wright et al., 2011; Vogel et al., 2016; Ploeger et al., 2017).

Generally, ~~an~~ enhanced isentropic STE between the extratropics and tropics is caused by the monsoon systems, in particular by the ASM during NH summer (Dunkerton, 1995; Chen, 1995). Haynes and Shuckburgh (2000) showed that, indeed, the subtropical jet acting as a transport barrier between the extratropics and tropics weakens during NH summer. Consequently, enhanced isentropic transport occurs in both directions, out of the tropics and from the extratropics into the tropics (termed in-mixing, in the following). Related stratospheric signatures can be found in the Tropical Tropopause Layer (TTL) as diagnosed from ~~the NASA's~~ NASA Aura Microwave Limb Sounder (MLS) observations of HCl and ozone (Santee et al., 2011, 2017). This in-mixed ozone contributes to more than half of the annual cycle of ozone in the upper part of the TTL (Konopka et al., 2010; Ploeger et al., 2012). Enhanced quasi-isentropic transport from the tropics to the midlatitude lowermost stratosphere driven by the ASM is also clearly observed both for tracers and water ~~vapor (Ploeger et al., 2013; Müller et al., 2016; Vogel et al., 2016; ?)~~ (Ploeger et al., 2013; Müller et al., 2016; Vogel et al., 2016; Rolf et al., 2018)

A regionally-resolved view on the processes coupling ENSO with the stratosphere, mainly during the winter and spring, has been adopted in several previous studies (Krüger et al., 2008; Liess and Geller, 2012; Garfinkel et al., 2013; Konopka et al., 2016). However, there are only a few publications investigating the impact of ENSO on the ASM anticyclone and on the related STE (Ju and Slingo, 1995; Kawamura, 1998; Wang et al., 2013). This is in contrast with a large number of investiga-

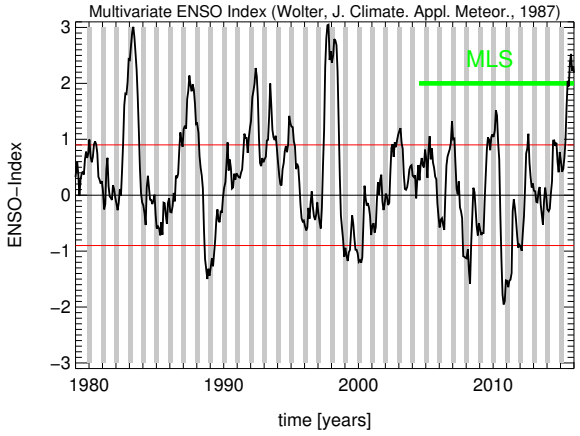

Figure 1. Multivariate ENSO Index (MEI) from the NOAA Climate Diagnostic Center, http://www.esrl.noaa.gov/psd/enso/mei ~~,~~ (Wolter, 1987). The red lines denote the threshold values (± 0.9) defining the El Niño (positive) and La Niña (negative) composites as used in this paper. ~~Gray~~ Grey shading shows winter seasons (December-February, DJF). As in Konopka et al. (2016).

tions connecting ENSO with the tropospheric variability of the ASM~~like weather patterns or~~ , such as weather patterns and precipitation, which have a long tradition starting with the pioneering studies of Walker (1923) and Bjerknes (1969).

In this study, we investigate how the ENSO winter signal propagates into the following seasons. In particular, we characterize the impact of ENSO on the upper branches of the Walker and Hadley circulation in the UTLS. We focus on the ASM anticyclone, its strength as well as its efficiency for in-mixing of stratospheric ozone into the TTL. We investigate how long ~~ENSO related statistically relevant~~ through the year ENSO related differences can last in the TTL both in the meteorological reanalysis as well as in long-term satellite, Lagrangian model and in-situ ozone ~~observations~~data. Section 2 discusses data and methods for our analysis. Section 3 describes the seasonal propagation of ENSO anomalies. Section 4 quantifies the influence of ENSO anomalies on the seasonality of ozone in the TTL. ~~Finally, section~~ Section 5 provides the ~~summary and~~ discussion. The last section gives the conclusions.

2 Data and methods

There are several indices to indicate the phase of ENSO, and they are highly correlated (Pumphrey et al., 2017). Here, the Multivariate ENSO Index (MEI, Fig. 1) from the NOAA (National Oceanic and Atmospheric Administration) Climate Diagnostic Center, http://www.esrl.noaa.gov/psd/enso/mei, is used to quantify the ENSO variability ~~(Wolter, 1987)~~(Wolter and Timlin, 2011). MEI is calculated based on sea surface pressure, zonal and meridional components of the surface wind, SST and total cloudiness fraction of the sky over the tropical Pacific. The two phases of ENSO typically show pronounced features in late fall, winter and early spring (Moron and Gouirand, 2003; McPhaden, 2015). Correspondingly, MEI shows peak ~~value~~ values during this period. Negative and positive values of MEI quantify La Niña and El Niño events, respectively.

La Niña			El Niño		
Year	Months	QBO	Year	Months	QBO
881988/89 1989	DJF	W	791979/80 1980	D	E
981998/99 1999	DJF	E	821982/83 1983	DJF	W
991999/00 2000	DJF	W	861986/87 1987	DJF	E
072007/08 2008	DJF	E	871987/88 1988	DJ	W
102010/11 2011	DJF	W	911991/92 1992	DJF	E
112011/12 2012	DJ	W/E	921992/93 1993	F	W
			941994/95 1995	DJF	E/W
			971997/98 1998	DJF	W
			022002/03 2003	DJF	W
			062006/07 2007	DJ	W
			092009/10 2010	DJF	E
			152015/16 2016	D	W

Table 1. List of all relevant La Niña and El Niño winter months during the period of 1979-2015. In total there are 17 and 28 months for the La Niña and El Niño composites, respectively, which are listed above (D/J/F for December, January and February). Within the La Niña composite there are 7 months in the easterly phase (E) and 10 months in the westerly phase (W) of the QBO (defined by 30 day smoothed equatorial wind at 50 hPa). For El Niño composites 11 months are in the easterly phase and 17 months in the westerly phase. The underlined years mark the long-lasting El Niño episodes (for details, see text). As in Konopka et al. (2016).

Hereafter, we define two winter composites (December-February, DJF) of ENSO events by the condition MEI< -0.9 for La Niña and MEI>0.9 for El Niño (red lines in Fig. 1) as discussed in Konopka et al. (2016). The winter months defining these two composites (17 ~~for~~ months for 6 La Niña events and 28 ~~for~~ months for 12 El Niño) are listed in Table 1. The quasi-biennial oscillation (QBO) phase during the considered months is also listed (http://www.cpc.ncep.noaa.gov/data/indices/qbo.u50.index) and shows that our composites are only weakly biased by the westerly phase.

El Niño episodes which last over the whole following year, are selected as the special long-lasting El Niño cases and underlined in Table 1 with black color (like during 1987 and 1992). The exceptional El Niño in 1982, which starts in spring 1982 and lasts until fall 1983, is also considered as a long-lasting El Niño case (underlined with dashed black in Table 1). These 3 cases as well as the influence of QBO on the results will be separately discussed in section 5.

~~The QBO phase during the considered months is also listed (https://www.esrl.noaa.gov/psd/data/correlation/qbo.data) and shows that our composites are only weakly biased by the westerly phase.~~

To study the effect of strong ENSO winters on the UTLS in the following months, we also consider climatologies of "shifted" composites for different seasons ~~, e.g.,~~ (DJF, JFM, FMA, MAM, AMJ, MJJ, and JJA), e.g., AMJ represents 4 months after ENSO winters (DJF). The mean value of a composite is defined from the averaged monthly means of its elements. Monte

Carlo significance test is used to investigate whether the La Niña and El Niño composites are statistically different or not. Monte Carlo significance test procedures consist of the comparison of the observed data with random samples generated in accordance with the hypothesis being tested (Hope, 1968). We call two (La Niña and El Niño) composites statistically different when the significance Monte Carlo test for their difference is passed at a 95% confidence level after at least 1000 iteration steps.

To quantify ENSO anomalies in the climatological flow patterns, stream function (SF) ψ and velocity potential (VP) χ are calculated (Tanaka et al., 2004) using meteorological data from ERA-Interim reanalysis during 1979-2015 (Dee et al., 2011). According to the Helmholtz theorem, an arbitrary 2D horizontal flow $\mathbf{u} = (u, v)$ can be separated into a non-divergent (i.e. rotational) part $\mathbf{u_a}$ with $\nabla \cdot \mathbf{u_a} = 0$ and a divergent (i.e. irrotational) part $\mathbf{u_b}$ with $\nabla \times \mathbf{u_b} = 0$, i.e.,

$$\mathbf{u} = \mathbf{u_a} + \mathbf{u_b} = \mathbf{k} \times \nabla\psi + \nabla\chi\,, \tag{1}$$

where both parts can also be expressed in terms of the potentials ψ and χ. Here, $\mathbf{k}$ denotes the unit vector perpendicular to the considered 2D surface. SF and VP are scalar quantities which are easy to plot and widely applied in meteorology and oceanography to represent large scale flow fields (see e.g., Evans and Allan, 1992; Kunze et al., 2016). SF quantifies the position and strengths of the cyclones and anticyclones. Following Tanaka et al. (2004), we use VP to represent the Walker circulation and the zonal mean of VP to quantify the Hadley circulation. SF and VP will be divided into El Niño and La Niña composites as described above~~for this study~~.

~~To~~ Ozone distributions are used to validate our diagnostic of the flow and to understand the effect of ENSO on the atmospheric composition in the UTLS region~~, ozone distribution is used to represent the influence~~. MLS ozone data (version 4.2) and the Hilo (Hawaii) ozonesonde data from Southern Hemisphere ADditional OZonesondes (SHADOZ~~) (Thompson et al., 2007)~~, Thompson et al. (2007)) are used (see http://croc.gsfc.nasa.gov/shadoz) as references. MLS measurements provide 8/6 months of data for the 3/3 La Niña/El Niño ~~composites~~ episodes from 2004 to 2015. Respectively there are 14~~and~~ /11 months of data for the 5/5 La Niña~~and~~ /El Niño ~~composites from SHADOZ ozondesonde~~ events from SHADOZ ozondesondes covering the period 1998-2015. Chemical Lagrangian Model of the Stratosphere (CLaMS) simulations (McKenna et al., 2002; Konopka et al., 2004; Pommrich et al., 2014) driven by the ERA-Interim reanalysis are used to obtain robust statistical composites of ozone (with the same number of La Niña/El Niño months ~~like~~ as for SF and VP). Outgoing long-wave radiation (OLR) monthly data from NOAA during 1979-2015 complete our analysis as a proxy for deep convection ~~(see http~~ (see https://www.esrl.noaa.gov/psd/~~enso~~data/~~mci~~gridded/data.interp_OLR.html).

3 ENSO anomalies at the tropical tropopause from winter to summer

In this section, we use the composites of the stream function (SF) and the velocity potential (VP) introduced above to illustrate some ENSO-related differences in the mean flow properties around the tropical tropopause.

3.1 Cyclones and anticyclones

Seasonal variations of SF after strong La Niña and El Niño winters are shown in Fig. 2. Here, respective climatologies are plotted at the potential temperature level θ=380 K, which roughly marks the tropopause in the tropics and ~~separates the overworld~~ in the extratropics separates the overworld from the lowermost stratosphere (Holton et al., 1995; Gettelman et al., 2011). The panels in Fig. 2 start from the winter (top, DJF) and end with the summer distribution (bottom, JJA).

Because the divergent part of the flow at θ=380 K is very small compared to ~~the rotational partof the flow~~its rotational part, isolines of SF approximate the climatological streamlines whereas strongest horizontal gradients of SF describe the highest flow velocities.The anticyclones are represented by ~~its~~ positive and negative SF values in NH and ~~SH~~ Southern Hemisphere (SH), with highest and lowest values corresponding to their centers, respectively. During DJF, the flow in the tropical UTLS between 60° E and 120° W is dominated by two equatorially symmetric anticyclones resembling the well-known (symmetric) Matsuno-Gill solution with the heat source from convection located symmetrically over the equator (Matsuno, 1966; Gill, 1980; Highwood and Hoskins, 1998).

The climatological sources of heat can be approximated by the lowest values of the OLR~~using the same type of composites like for SF (white~~. The analogous composites for OLR (magenta contours in Fig. 2) as for the SF are built with respect to La Niña and El Niño conditions. Thus, following the symmetric Matsuno-Gill solution as a proxy, the relevant latent heat sources for the anticyclones originate mainly in the western Pacific, especially during La Niña, and these sources are partially shifted to the east ~~,~~ during El Niño events.

Over the course of the following 6 months, as the ~~ITCZ~~ inter-tropical convergence zone (ITCZ) moves northwards, these two anticyclones shift to the north-west roughly following the position of convection (Highwood and Hoskins, 1998). The anticyclone in the NH intensifies, starting in May and June, and forms the well-known Asian summer monsoon (ASM) anticyclone during NH summer. In addition a weaker anticyclone in the ~~Southern Hemisphere~~ SH can also be diagnosed. Thus, the summer configuration resembles more a superposition of a symmetric and ~~asymmetric~~ anti-symmetric Matsuno-Gill solution ~~(Zhang and Krishnamurti, 2006)~~(Gill, 1980; Zhang and Krishnamurti, 2006).

Now we discuss the differences in the large-scale flow in the UTLS caused by ~~the~~ ENSO (i.e. differences between the left and the right column of Fig. 2). The most striking difference in DJF is a much weaker meridional disruption of the subtropical jets during El Niño than during La Niña winters, mainly in the NH subtropics between 170° E and 70° W. At the lower levels (not shown), such stratospheric intrusions coincide with regions of the so called "westerly ducts", which are much weaker during El Niño (Waugh and Polvani, 2000).

Furthermore, the equatorially symmetric anticyclones are more pronounced for the La Niña composites due to ~~a stronger~~ stronger and more localized convection in the western Pacific. These differences are also present during FMA, become smaller during AMJ and disappear during JJA mainly because forcing of the summer dynamics, especially of the ASM, is only weakly related to the winter forcing.

The mean climatological anticyclone in AMJ ~~is similar to the~~ (Fig. 2) is at the very beginning phase of ASM anticyclone after El Niño winters, while it ~~is closer to the mature phase~~ develops quickly and becomes stronger after La Niña winters.

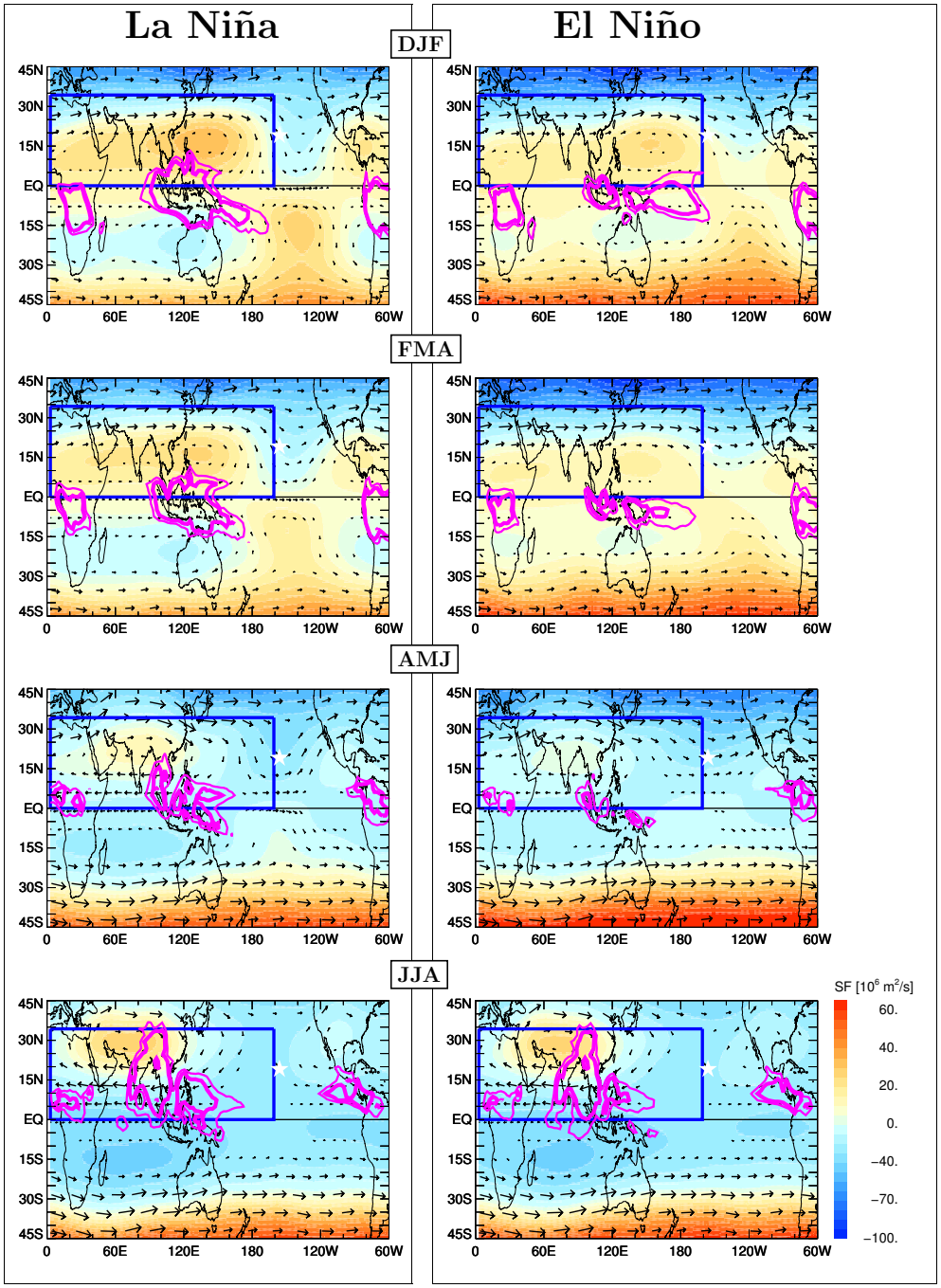

Figure 2. Climatologies (composites) of the stream function (SF, in 10^6 m^2/s) at θ=380 K calculated from ERA-Interim (1979-2015) for months following La Niña (left) and El Niño (right) ~~winter~~ winters until summer (from top to bottom). The arrows represent the rotational horizontal wind. ~~White~~ Magenta isolines indicate the strong convection regions based on OLR (thick and thin lines represent 210 and 220 W/m^2 contours~~) data~~, respectively). The blue rectangles mark the locations of strong anticyclone in NH (for details, see text). Hereafter, the star in the figure marks the location of the SHADOZ station ~~used in this study~~ (Hilo, Hawaii) where long-term ozonesonde observations are available (see section 4.3).

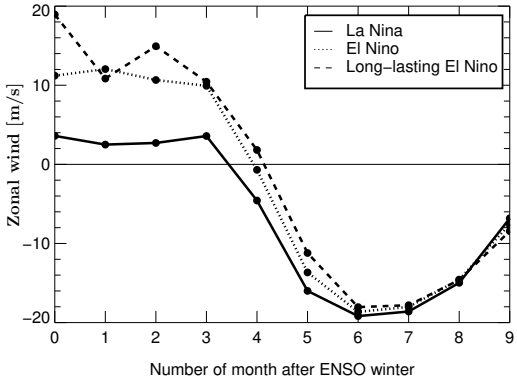

Figure 3. Mean zonal wind in the tropics over south-east Asia ([5° N, 20° N; 40° E, 120° E]) following La Niña, El Niño, and long-lasting El Niño winters at 200 hPa. The transition from positive to negative values marks the onset of the Asian summer monsoon (ASM). The zero mark on the x-axis denotes the middle of the DJF season (i.e., 15 January).

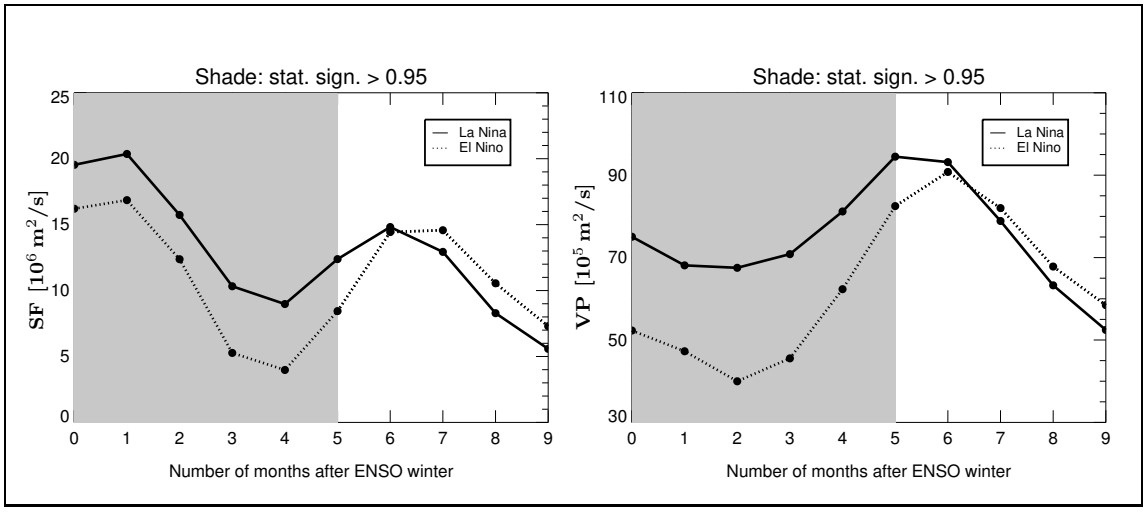

Figure 4. The average value of the stream function (left~~, in 10^6 m^2/s~~) in the domain of [0° N, 35° N; 0° E, 160° W] and velocity potential (right~~, in 10^5 m^2/s~~) in the domain of [~~20~~30° S, 40° N; 90° E, 140° W] for La Niña (solid line) and El Niño (~~dot~~ dotted line) composites at θ=380 K. The ~~dashed~~ grey shading region denotes ~~a~~ the period with statistically significant differences between the two composites.

We use the transition of the upper-level (at 200 hPa) flow from westerly to easterly over south-east Asia [5° N, 20° N; 40° E, 120° E] to characterize the onset of the monsoon as ~~used~~ discussed in Ju and Slingo (1995). ~~It~~ By using the shifted composites as in the previous section, it turns out that the onset of the ASM after La Niña is about a half month earlier than after El Niño (Fig. 3). The difference in SF between La Niña and El Niño composites lasts from winter (DJF) to early summer (AMJ) and becomes insignificant in summer (JJA) as noted earlier.

To prove the statistical significance of the ENSO anomalies in the SF composites, we compare their mean values averaged over a representative region shown as a blue rectangle in ~~Figs~~Fig. 2. The domain, defined as [0° N, 35° N; 0° E, 160° W], contains the NH anticyclone from winter to summer. The results are shown in the left panel of Fig. 4. The period with statistically different composites is grey ~~hatched~~shaded. Thus, the NH anticyclone in La Niña years is significantly stronger than in El Niño years within the first 5 months of the year, i.e. until MJJ. This statistical analysis indicates that the influence of ENSO on the anticyclone propagates from winter until early summer. The mean SF difference between La Niña and El Niño composites from winter to early summer is $\sim 6 \times 10^6\,\mathrm{m}^2/\mathrm{s}$.

3.2 Walker circulation

Complementary to SF, the divergent part of the horizontal flow can be described by the velocity potential VP and is shown in Fig. 5. Note that VP is a factor of 10 smaller than SF, which is consistent with the fact that the non-divergent rather than divergent part dominates the flow at θ=380 K. Following Tanaka et al. (2004), the positive peak of VP indicates the intensity of the Walker circulation and the zonal mean of VP ($\overline{\mathrm{VP}}$) quantifies the Hadley circulation (see below). The positive values of VP represent divergence or, using the continuity equation, the strength of upwelling, while the negative values are related to convergence or downwelling. In this way, the upper branch of the Walker circulation can be diagnosed in Fig. 5. The intensities of the Walker circulation are similar to the results from Tanaka et al. (2004).

The positive peak values of VP lie in the western and central tropical Pacific for La Niña and El Niño DJF climatologies, respectively. They correspond to the locations of rising motion. The mean upwelling (downwelling) activity in La Niña winters is much stronger than in El Niño winters, in agreement with the well-known weakening of the Walker circulation after El Niño events (Wang et al., 2002). In spring (FMA) ~~these differences~~ the differences between the two composites become smaller than in winter~~for both composites~~. At the beginning of summer (AMJ), the centers of the divergence start to shift from the tropics to the extratropics and the differences become even smaller. In JJA, these centers reach the China Sea. The strength and position of the convergence/divergence centers in the La Niña composite ~~is comparable with that~~ are comparable to those of El Niño in that season.

~~Similarly as~~ As was done for SF, the statistical significance of the ENSO anomalies in the VP composites is diagnosed in the right panel of Fig. 4. The ~~mean values over the~~ blue rectangle in Fig. 5, defined as [~~20~~30° S, 40° N; 90° E, 140° W], represents the region of the ascending branch of the Walker circulation. The mean positive values over this blue rectangle are calculated. The domain ~~quantifies~~ allows quantification of the average upwelling of the Walker circulation. The divergence in the La Niña composite is significantly higher than in the El Niño composite within the first 5 months of the year. The mean VP difference between La Niña and El Niño composites from winter to early summer is $\sim 22 \times 10^5\,\mathrm{m}^2/\mathrm{s}$.

3.3 Hadley circulation

The zonal mean of VP ($\overline{\mathrm{VP}}$) is used to represent the Hadley circulation (Fig. 6 ~~, top~~(a) and (b)). Note that the peak values of VP are more than three times larger than $\overline{\mathrm{VP}}$. In winter, ~~the zonal mean of VP~~ $\overline{\mathrm{VP}}$ is positive in SH and negative in NH. The positive peaks represent the locations of rising air and correspond to the ~~inter-tropical convergence zone (ITCZ)~~ITCZ. The negative

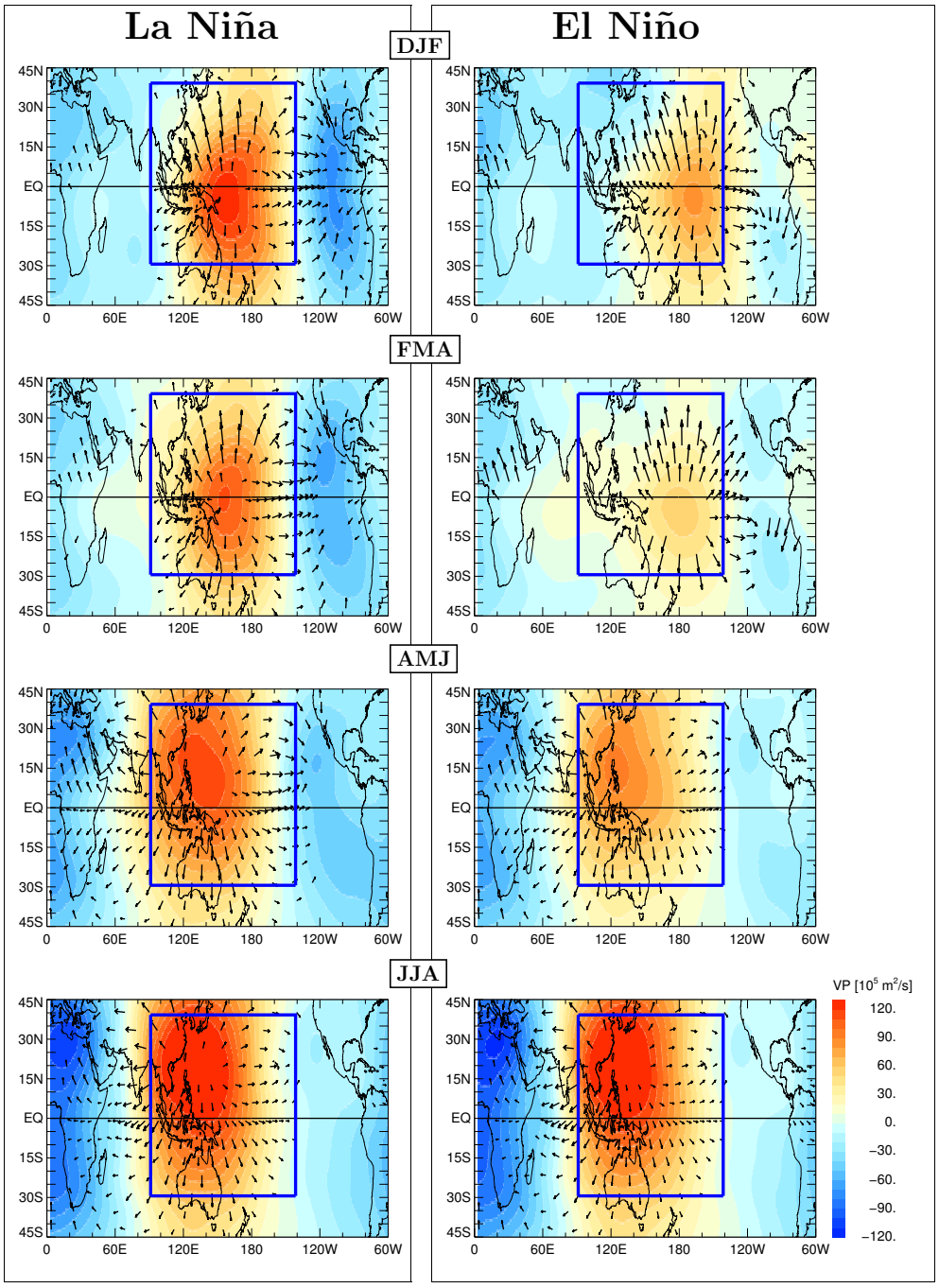

Figure 5. Same as Fig. 2 but for the velocity potential VP (in 10^5 m^2/s) at θ=380 K with arrows denoting the divergent part of the horizontal wind.

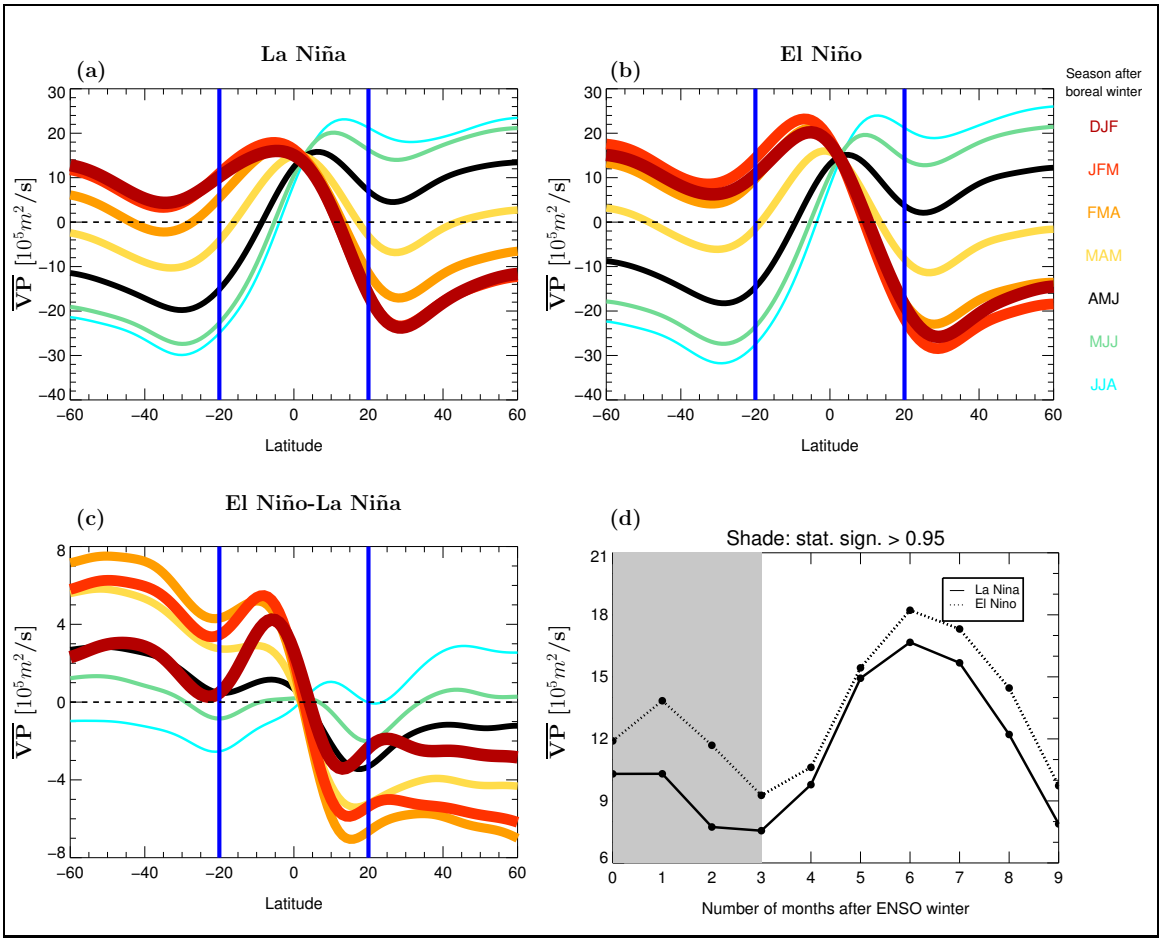

Figure 6. Zonal mean of the velocity potential at θ=360 K defining the Hadley circulation and calculated for La Niña (a) and El Niño composites (~~top~~b). The difference between La Niña and El Niño composites (c). The average intensity of Hadley circulation calculated for the domain of [20° S, 20° N] (~~bottom~~d).

peaks represent the locations of sinking air. The rising and sinking motions form the mean meridional Hadley circulation. This circulation is weaker after La Niña than after El Niño ~~with decreasing ENSO differences from DJF to JJA~~episodes, and the differences between the La Niña and El Niño composites decrease in summer.

The latitudes of positive peaks show that the rising motion is shifted southwards after El Niño winters compared to La Niña winters. Correspondingly, the ITCZ is located around 4° S and 6° S for the La Niña and El Niño composites, respectively. Fig. 6 (c) shows the difference between La Niña and El Niño composites. The upwelling and downwelling after El Niño is much stronger than after La Niña from DJF to MAM. The difference becomes smaller after AMJ. To check the statistical significance of such differences, the average rising intensity of the Hadley circulation~~in~~, which is located in the tropics (from 20° S to 20° N), is calculated (Fig. 6 ~~, bottom~~(d)). The values after El Niño winters are ~~stronger~~ higher than after La Niña winters, especially ~~during DJF and MAM~~ from DJF to MAM as noted before. The mean difference is about 2×10^5 m^2/s, and becomes insignificant starting from April.

4 Impacts on ozone distribution

So far we have investigated the influence of ENSO anomalies on the atmospheric circulation, especially on the mean horizontal flow quantified in ~~term~~ terms of the stream function SF (Fig. 2) and velocity potential VP (Fig. 5). Such changes of the atmospheric circulation will also affect the distribution of atmospheric constituents (Randel et al., 2009; Ziemke et al., 2015). Ozone is a sensitive indicator of transport properties in the UTLS region due to its strong vertical and horizontal gradients and its relatively long chemical lifetime. Furthermore, in the sub- and extratropics around the subtropical jet, the ozone distribution is mainly determined by transport rather than by chemistry. In this section, we quantify the impact of ENSO anomalies on the mean ozone distribution based on MLS satellite data, CLaMS simulations and SHADOZ ozonesonde data.

Particularly, we investigate now the influence of ENSO on the isentropic in-mixing of high stratospheric ozone values into the tropical TTL ~~is investigated~~ (Konopka et al., 2010). In the following, the ozone isoline at the tropopause is used to quantify the effect of isentropic in-mixing at ~~380~~$\theta = 380$ K~~potential temperature~~. Thouret et al. (2006) estimated the monthly mean climatological ozone concentration at the tropopause based on MOZAIC measurements. They found a maximum value in May (120 ppbv) and a minimum value in November (65 ppbv). Here, the isoline of 120 ppbv is used as the ozone boundary for CLaMS composites to obtain a conservative estimate of stratospheric influence. MLS ozone is high biased by ~40% at 100 hPa in the tropics ~~(?)~~ (Livesey et al., 2017) and even by as much as ~70% inside the ASM anticyclone (Yan et al., 2016). ~~The precision of MLS ozone at tropopause is about 40 ppbv (Livesey et al., 2017).~~ Therefore, the isoline of 185 ppbv is used as a proxy ~~at~~ for the tropopause in the MLS composites.

4.1 MLS composites

~~Fig.~~Figure 7 shows MLS ozone mixing ratio distributions at θ=380 K from winter to summer after La Niña and El Niño winters. The ozone isoline at the tropopause is represented by the black solid line. During DJF and FMA, the El Niño composite is more zonally symmetric compared to La Niña. This is consistent with the ~~zonally symmetric pattern of the SF in~~ less disturbed

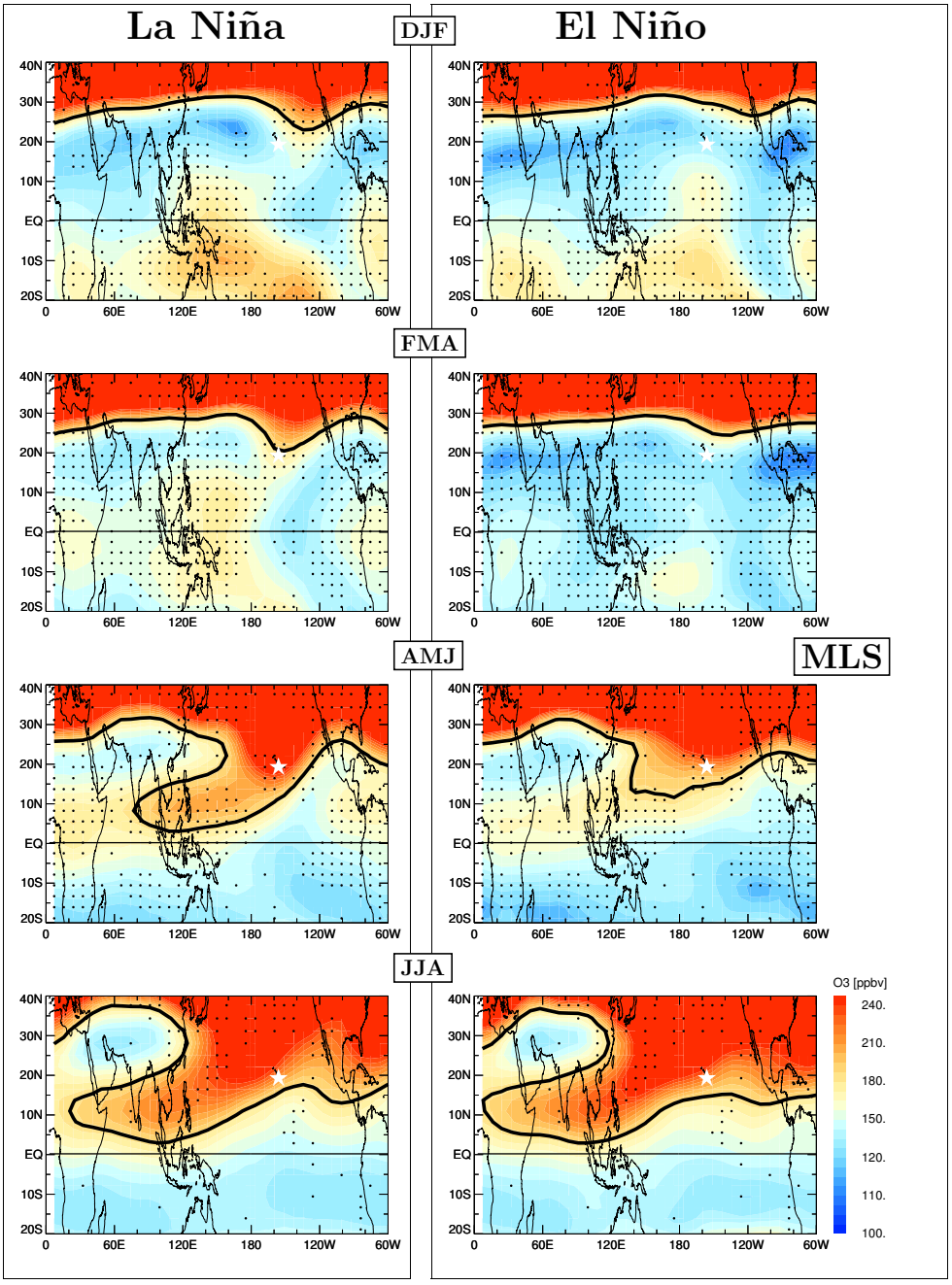

Figure 7. Seasonal ozone climatology derived from MLS observations (2004-2015, version 4.2) at θ=380 K for La Niña and El Niño composites from winter to summer months (from top to bottom). ~~The~~ Regions with statistically significant ~~regions~~ differences are marked by the black dots. The black isolines represent ozone ~~at tropopause with~~ of 185 ppbv, which mark the tropopause (see text).

subtropical jets after El Niño winters as discussed in the last section. The region of enhanced in-mixing can be recognized as a tongue of high ozone which emerges around 120° W, 30° N during DJF and is shifted in the following months to the west until the ASM anticyclone forms.

During AMJ, this feature of in-mixing is much more pronounced for the La Niña than for the El Niño composite. This may be related to the differences in the ~~phase~~ developing process of the ASM anticyclone between La Niña and El Niño shown in Fig. 2. The mean anticyclone in AMJ ~~show similar feature to the ASM anticyclone in the~~ is at the very beginning phase after El Niño, while ASM anticyclone after La Niña ~~is close to the mature phase~~ develops more quickly and the ozone distribution is affected by stronger ASM anticyclone during this period. The largest pattern difference between La Niña and El Niño ozone composites occurs during this period, while the SF shows the largest pattern difference in winter (Fig. 2, top). Ozone in-mixing anomalies seem to be delayed compared to the distribution of SF.

The black dots in Fig. 7 provide the information about regions with statistically significant differences between La Niña and El Niño composites. ~~Thus, such differences mainly exist~~ We can see that the differences exist almost everywhere, especially in the regions of strong in-mixing described above. During the mature phase of the ASM anticyclone (JJA), the ~~significantly different regions between La Niña and El Niño composites decrease strongly~~number of black dots decreases strongly, but there is still a region of significant in-mixing differences on the ozone tongue as well as the extratropical side of the tropopause. We will return to this point later. Ozone values in the center of the ASM anticyclone are lower after La Niña than after El Niño ~~winters~~ in JJA which is consistent with the similar differences in ~~SF and VP~~ the SF (c.f. Fig. 2~~and Fig. 5~~).

The isolines of ~~the ozone at~~ ozone representing the tropopause are combined together in Fig. 8 (a) and (b) to illustrate the pattern of the seasonality of the ENSO-related differences in in-mixing. To quantify such differences, the mean concentration inside the blue domain [0° N, 25° N; 60° E, 120° W] is calculated and shown in ~~the bottom panel of~~ Fig. 8 (c). The ~~dashed lines represent the significantly different seasons~~ grey shading highlight the seasons with statistically significant differences between La Niña and El Niño composites, which are from DJF to AMJ. The average results inside the ~~in-mixing~~ in-mixed region attest that ozone concentration after El Niño is about 16 ppbv lower than after La Niña from winter (DJF) to early summer (AMJ). The difference ~~manifests~~ is a manifestation of the influence of stronger Hadley/~~BD-circulation~~ BD circulation and weaker in-mixing after El Niño than after La Niñ~~o (Randel et al., 2009; Calvo et al., 2010; Konopka et al., 2016) on ozone horizontal distribution around tropopause~~a on the horizontal distribution of ozone around the tropopause (Randel et al., 2009; Calvo et al., 2010; Konopka et al., 2
Starting from summer, the difference of ozone distribution between El Niño and La Niña becomes ~~insignificant.~~ statistically insignificant. Starting in JJA, the concentration of in-mixed ozone after El Niño years is even higher than after La Niña years.

To understand better such statistical differences, we investigate now in more detail the MLS observations for three example years which are representative of "typical" El Niño, La Niña and neutral conditions. Following the method described in Santee et al. (2017), we plot in Fig. 9 the time series of the zonally averaged ozone (10° – 130°E) at 380 K during 2008 (i.e. after La Niña), during 2009 (i.e. during a neutral year) and during 2010 (i.e. after El Niño). Over the course of these three representative years, the differences in ozone between the equator and ~30° N mainly result from different intensities of in-mixing and of the BD-circulation. Specifically, the ozone mixing ratios after El Niño winter (2010) are much lower than after La Niña winter (2008) or even during a normal year (2009), with a negative anomaly persisting from January to June,

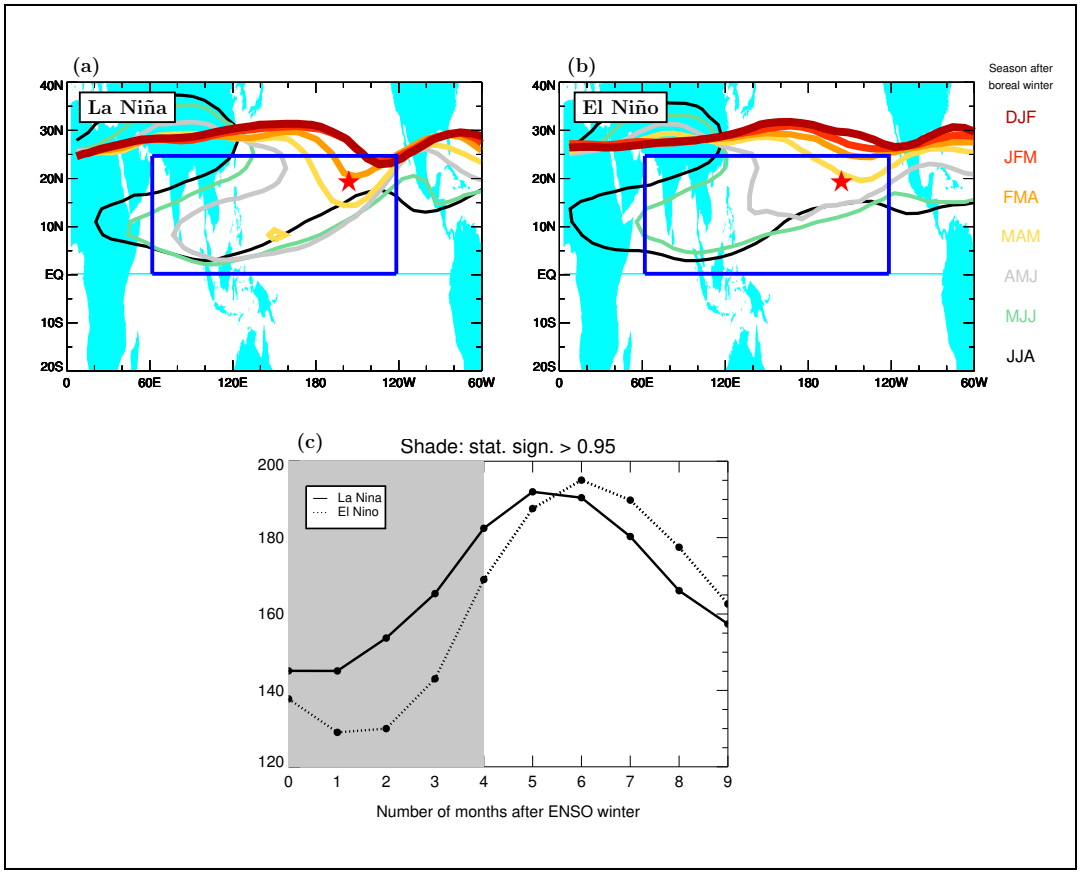

Figure 8. Top: Isolines of MLS ozone (185 ppbv, black lines in Fig. 7) approximating the tropopause at θ=380 K for different seasons following La Niña (a) and El Niño (b) winters (from DJF (red) to JJA (~~grey~~black)). Bottom: The mean concentration of ozone from the blue domain in the top panel ([0° N, 25° N; 60° E, 120° W]) marking the region of strongest ENSO-related differences in in-mixing (c).

supporting our statistical results in Fig. 7 and Fig. 8. The isentropic intrusions transport less ozone from high latitudes to the tropics following El Niño winters.

However, there is more in-mixed ozone in 2010 than in 2008 and 2009 from June to September. This could be a consequence of the differences in the BD-circulation (stronger after El Niño than after La Niña winters), which may cause higher ozone values in the northern extratropics and, consequently, stronger isentropic gradients of ozone after El Niño winters. It means that under El Niño conditions, transport of ozone-rich air from the extratropics to the tropics is inhibited during winter and spring by the strong subtropical jet, but such transport to the tropics may occur later in summer when the subtropical jet is weaker. We will come back to this point in section 5.

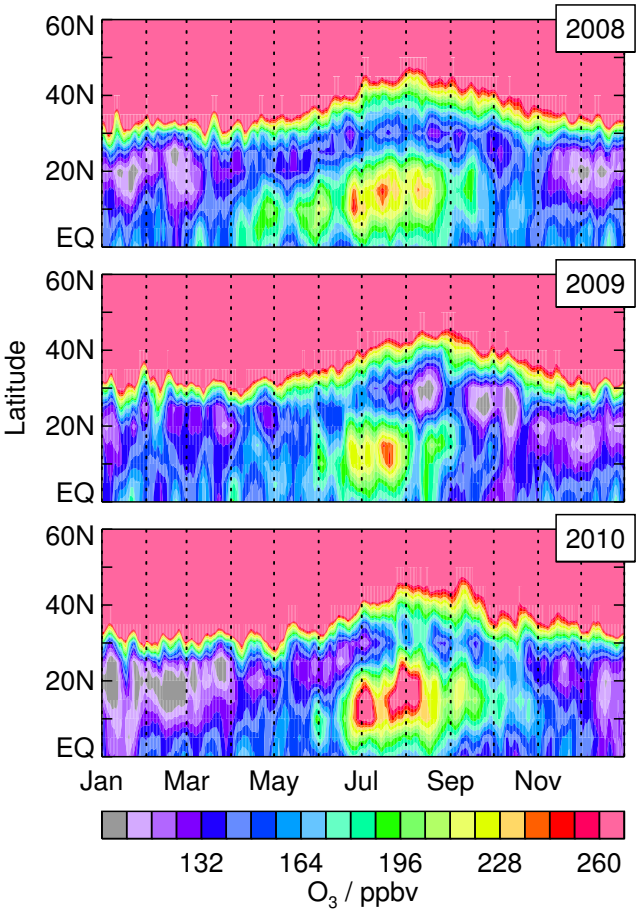

Figure 9. Zonally averaged (10° – 130° E) time series of MLS ozone at $\theta = 380$ K (version 4.2, for more details see Santee et al. (2017)) over the course of these 3 representative years (top to bottom): 2008 (after La Niña winter), 2009 (a normal year) and 2010 (after El Niño winter).

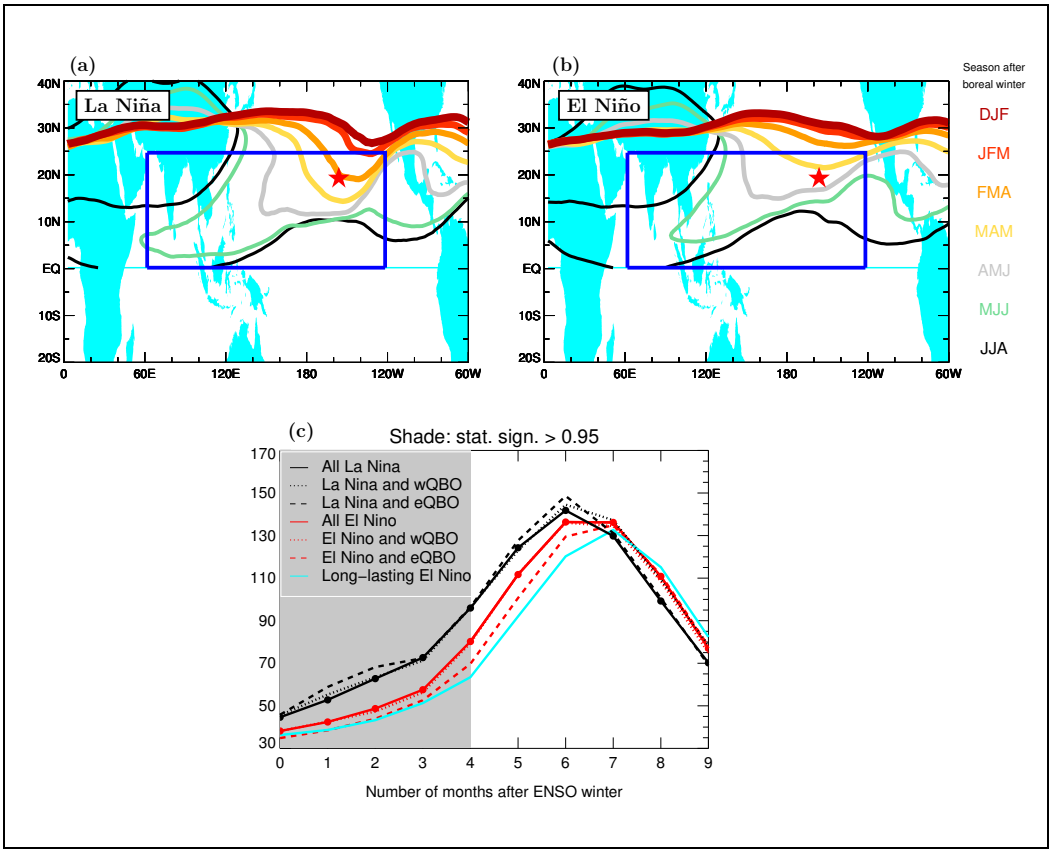

Figure 10. Top: Same as Fig. 8 but for CLaMS ozone with the isoline value of 120 ppbv. Bottom: Same as Fig. 8 (c) but including also the results for ENSO subcomposites with QBO westerly phase (dotted line), QBO easterly phase (dashed line) and long-lasting El Niño events (cyan line).

4.2 In-mixing from CLaMS

As discussed in Konopka et al. (2016, Figure 5), CLaMS reproduces fairly well the ENSO anomalies in ozone observed by MLS. However, at the time of writing the MLS composites cover only 11 years with very few strong El Niño/La Niña events. Using CLaMS ozone, we are able to extend our period to 37 years from 1979 to 2015 and obtain ~~more statistically~~ statistically more robust results.

~~Fig.~~ Figure 10 (top) shows the same type of distribution ~~like~~ as Fig. 8 (top) but for 37-years of CLaMS ozone simulations ~~. The isolines represent the ozone at the tropopause~~ and with the tropopause defined by the ozone isoline with 120 ppbv. ~~They are used to characterize the ozone distribution after ENSO. The ozone concentration~~ The ozone concentrations from CLaMS simulations are about 50 ppbv lower than MLS measurements at θ=380 K~~for both La Niña and El Niño during all seasons partially~~, in part because of the zero ozone boundary condition at the ground, but they show similar patterns to MLS ozone.

The CLaMS ozone distributions also show in-mixing activity over eastern and central Pacific in subsequent months following La Niña winters, with more zonally symmetric features during months following El Niño. The signatures of in-mixing over the tropical Pacific become much stronger after the onset of the ASM anticyclone (AMJ) for both composites ~~. The ozone intrusion from high latitude into the TTL is deeper following~~ and extend deeper into the tropics after La Niña than ~~following~~ after El Niño winters. The differences disappear in JJA.

The largest difference between the ENSO composites exists around the eastern flank of the ASM anticyclone. To quantify this difference from CLaMS simulations, the mean ~~concentration~~ concentrations in the blue domain ~~(same~~ are calculated (i.e. in the same way as for MLS) ~~is calculated. The results are shown~~ and are shown as solid black and red lines in Fig. 10 (c) ~~. The significant difference between~~ for La Niña and El Niño ~~lasts from winter (DJF) to early summer (AMJ~~ composites, respectively (the results for the long-lasting El Niño years and for the subcomposites related to the different QBO phases are also shown and will be discussed in section 5). As for the MLS composites, the CLaMS results show a similar pattern with less in-mixed ozone after El Niño winters until early summer and more in-mixed ozone in the late summer and fall, although statistically significant differences can only be found until AMJ (grey shading). The ozone concentration after El Niño is about 12 ppbv lower than after La Niña. This difference obtained from CLaMS simulations for the time period ~~from 1979 to 2015~~ 1979-2015 is slightly smaller than from MLS measurements for the time period ~~from 2004 to 2015.~~ 2004-2015.

4.3 In-mixing from SHADOZ

MLS measurements and CLaMS simulations as described above provide the ENSO-related differences in the horizontal distribution of ozone. The vertical influence of ENSO anomalies on the ozone distribution near the tropopause can also be inferred from the ozonesonde data ~~observed~~ obtained at the SHADOZ station in Hilo, Hawaii [19.43° N, 155.04° W] (marked with a star in Fig. 2, Fig. 7, Fig. 8, and Fig. 10) from 1998 to 2015. Hilo is located in the central Pacific at the edge of the climatological position of the anticyclone in winter (see Fig. 2). The air over Hilo is strongly affected by the meridional disruption of the subtropical jet from winter (DJF) to early summer (AMJ) following La Niña winters, while it is within the tropics following El Niño winters.

The ~~SHADOZ ozonesonde data are used to investigate the vertical distribution of the ENSO-related anomalies. The~~ resolution of the SHADOZ ozone profiles is not the same for the whole period, so the data is degraded to the vertical resolution of 200 m for all the years to calculate the ~~statistical ozone profiles. The seasonal mean profiles following La Niña and El Niño winters are calculated for~~ ENSO composites introduced in section 2. ~~Fig.~~ Figure 11 shows the ENSO-related seasonal variation of ozone with altitude over Hilo ~~from winter (DJF) to summer (JJA) following ENSO~~ (red and black solid profiles), as well as their variability due to the QBO phase (dotted and dashed lines), which will be discussed in the next section.

The mean ozone profiles ~~following~~ during and after El Niño show a ~~common vertical~~ characteristic "S" ~~shape~~ -shape structure for all the seasons, with the lowest value near the surface, a maximum near 6 km, a minimum near ~~12~~12-13 km, and a subsequent increase toward stratospheric values. ~~However, the mean ozone profiles from La Niña do not exhibit this structure except for JJA. The low ozone concentrations of ≈ 30-40 ppbv at altitude of ≈ 12-14~~The minimum ozone concentrations at ~ 12-13 km

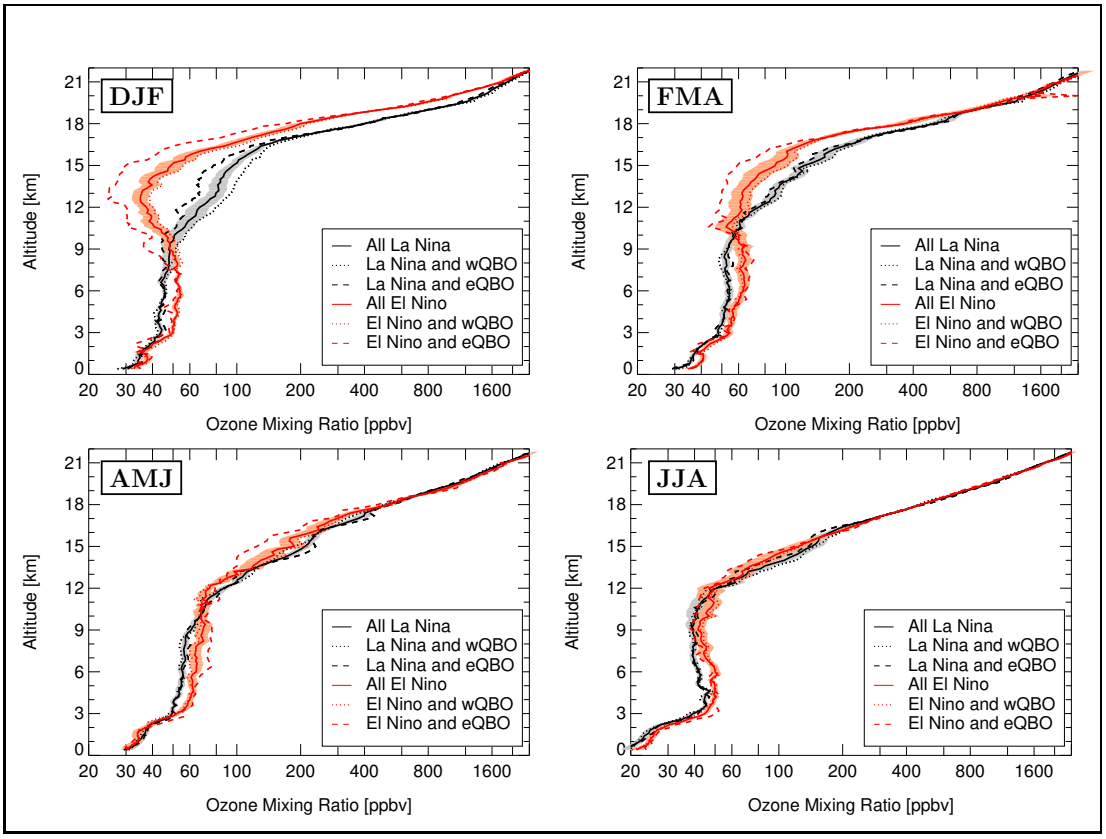

Figure 11. ~~Ozonesonde~~ Composites of the ozonesonde measurements from SHADOZ in Hilo, Hawaii [19.43° N, 155.04° W] during 1998-2015. Black and red lines represent the seasonal mean profiles for La Niña and El Niño composites, respectively. The ~~shade~~ shading indicates the standard deviation of the mean. The ~~location~~ dotted and dashed lines represent the results for subcomposites defined by the westerly and easterly phase of the ~~data used here is marked (star) in Fig. 2, Fig. 7, Fig. 8~~QBO, ~~and Fig. 10~~respectively.

~~after El Niño~~ are located at the level of main convective ~~out flow~~ outflow and are therefore caused by uplift of tropospheric air ~~by convection (Folkins et al., 2002; Thompson et al., 2012).~~

(Folkins et al., 2002; Thompson et al., 2012). On the other hand, the ozone profiles ~~after~~ from La Niña winters do not show ~~an "S" shape. Fig. 11 shows that the ozone concentration in the middle troposphere following La Niña is lower than after El Niño, which will be discussed below. In addition, the ozone concentration in the UTLS from DJF to AMJ following La Niña is higher than after El Niño~~such a minimum. On average, the ozone concentration for La Niña is about ~~110~~44 ppbv higher than for El Niño from 9 km to ~~21~~18 km in DJF (top left). The ozone concentration ~~difference~~ differences between La Niña and El Niño during FMA and AMJ (top right ~~) becomes smallerthan during DJF, when the mean difference is about 54 ppbv in the layer from 10 km to~~ and bottom left) are smaller, with mean values around 38 and 20 ~~km. The mean concentration of ozone~~

following La Niña is higher than following El Niño from 11 km to 18 km during AMJ (bottom left), the difference is about 28 ppbv. There ppbv, respectively. Finally, there is no clear difference between the two composites in the UTLS region these two composites during JJA (bottom right).

The results from SHADOZ indicate that the air masses are more affected by in-mixing following La Niña years, and the strong meridional disruption of the subtropical jet and in-mixing phenomenon after La Niña impact the air masses not only at that this effect is not only confined to the region around 380 K (≈ 15 km) but also throughout the can be diagnosed throughout the whole UTLS region. Especially in winter, ENSO anomalies have the strongest influence on ozone profile related anomalies in the ozone profile are quite large (from 9 km to 21 km) comparing to other seasons. The influence lasts from winter (DJF) to early summer (AMJ), but vanishes during summer (JJA)JJA. Interestingly, the ENSO anomaly of in-mixing changes sign in the middle troposphere below 9 km. We discuss this point in the following section.

Note that the ozone

5 Discussion

The ENSO anomaly induces two types of variability in the global ozone distribution: On the one hand, the stronger Hadley/BD-circulation during and after El Niño winters transports less ozone into the TTL and more ozone in the extratropical lower stratosphere and, consequently, stronger latitudinal gradients of ozone on all isentropes in the UTLS region have to be expected (Randel et al., 2009; Calvo et On the other hand, a less disturbed subtropical jet after El Niño is higher suppresses more effectively the isentropic in-mixing of ozone into the tropics during winter and spring (this effect was extensively shown in this paper), while during late summer and fall higher ozone values, although less frequently, can be in-mixed into the TTL.

The latter effect can be seen in the MLS observations at $\theta = 380$ K (Figure 9) mainly caused by isentropic in-mixing around the eastern flank of the ASM anticyclone. This effect can also be inferred from our statistical analysis of the enhanced mean ozone values in the blue region discussed in Figure 8. These values shown in Figure 8 and 10 for MLS and CLaMS, respectively, suggest that during late summer and fall the in-mixed ozone is higher after El Niño than after La Niña in the middle troposphere (winters, although we cannot prove the statistical robustness of this result. In addition, all the SHADOZ mean profiles around 3-9 km) from SHADOZ data (Fig. (Figure 11) . show higher ozone for El Niño than for La Niña composites.

To discuss this point in more detail, Figure 12 The zonal mean ozone anomalies in the west and central Pacific are calculated to understand the potential influence from ENSO. Fig. 12 shows shows from top to bottom the seasonal results of the zonal mean (120° E - 120° W) ozone anomalies after La Niña and El Niño from the surface to 70 hPa . The largest influence of ENSO on ozone occurs in the lower stratosphere, but the influence extends even downward into the middle troposphere. In DJF and FMA as derived from the respective CLaMS composites. The depicted ozone anomalies are mainly due to changes in the Hadley/BD-circulation, with the largest negative (positive) changes in the TTL and positive (negative) changes in the lower extratropical stratosphere mainly in the NH following El Niño , the figure indicates that the ozone in the tropics shows a negative anomaly from the surface to the tropopause, whereas the ozone in the subtropics shows a positive anomaly behind subtropical jet.However, it shows an opposite pattern following La Niña. This manifests that the enhanced upwelling in the

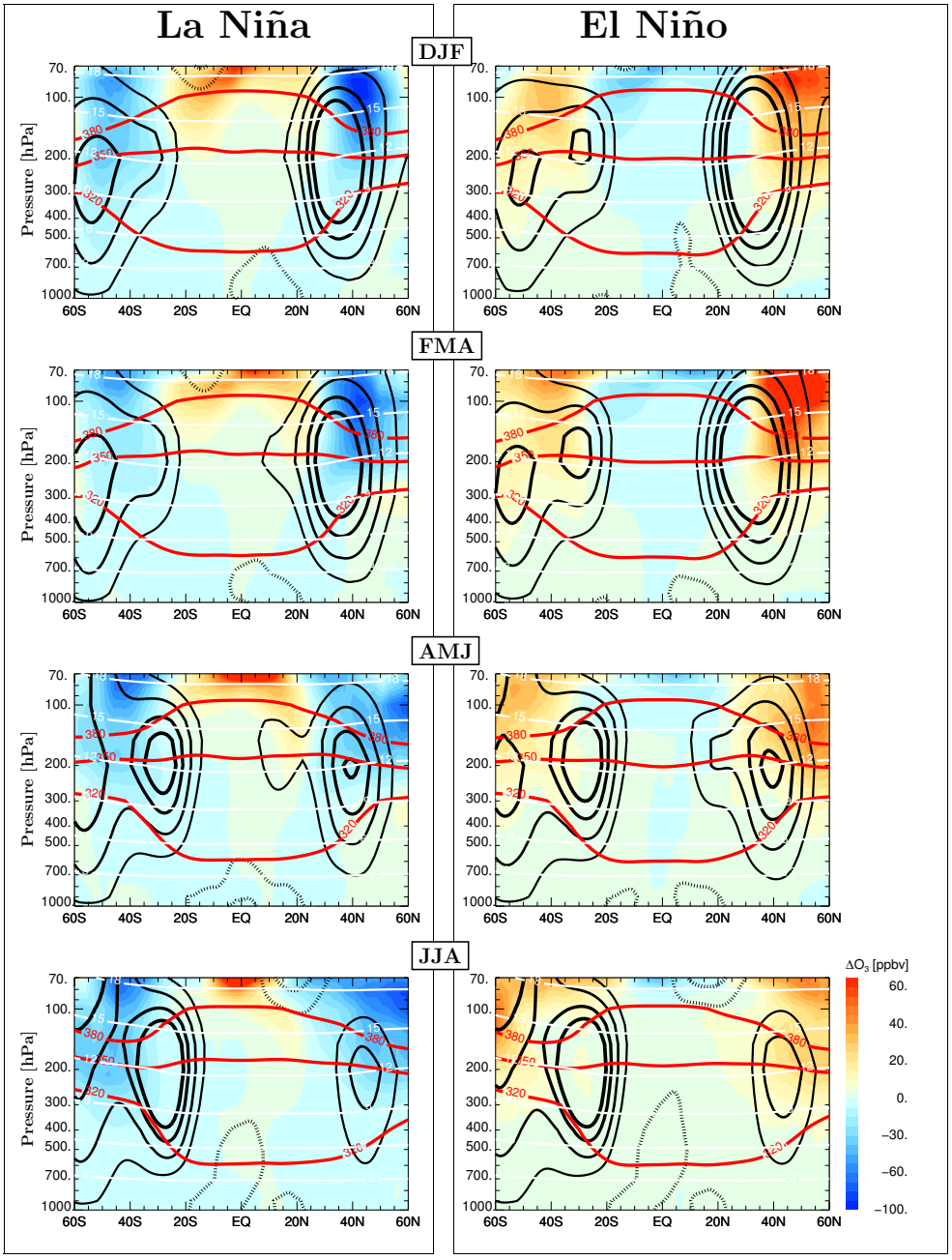

Figure 12. ~~Zonally~~ The anomalies of zonally averaged ozone ~~anomalies~~ in west and central Pacific [120° E, 120° W] from DJF to JJA based on CLaMS simulations covering 1979-2015. The solid and dashed lines are the zonal means of the westerlies (10, 17, 24, and 30 m/s) and easterlies (−5, −10, and −20 m/s), respectively. Red and white lines represent ~~θ=380~~ potential temperature (K~~level. White lines represent GPH~~) and geopotential height (km), respectively.

~~tropics in~~ (La Niña) winters. Although the largest ozone anomalies can be found in DJF and FMA, their absolute values weaken in the following months, especially in the tropics. In addition, the positive anomaly in the north of the subtropical jets (black lines in Fig. 12) under El Niño conditions propagates downwards into the middle troposphere, mainly in the NH.

We conclude that enhanced tropical upwelling in DJF and FMA following El Niño ~~can bring~~ transports ozone poor air from the surface to the ~~high altitude above the tropopause~~TTL. Likewise, the enhanced downwelling ~~polewards~~ poleward of the subtropical jets ~~(black lines in Fig. 12)~~ following El Niño ~~can transport~~ transports ozone rich air from the stratosphere to the sub- and extratropical middle troposphere. The higher ozone as observed by MLS at $\theta = 380$ K during late summer 2010 (Figure 9) as well as the higher ozone in the middle troposphere below 9 km in Hilo during DJF and FMA following El Niño (Figure 11) may be partially related to the isentropic transport of ozone-rich air from the stratosphere. ~~The stratospheric influence on the subtropical middle troposphere, affecting the "S" shape of ozone profiles, was suggested by ?Hayashi et al. (2008); ?); Neu et al. (2014). The difference becomes small in AMJ, and it disappears in JJA~~While in the first case, the isentropic transport happens above the jet, mainly on the eastern flank of the ASM anticyclone, in the second case the isentropic pathway of transport is related to the isentropes below the jet, i.e. to the θ surfaces between 320 and 340 K (Newell et al., 1999; Thouret et al., 2001; Hayashi et al., 2008; Pan et al., 2015).

6 ~~Discussion~~

Inspired by the work of Chowdary et al. (2016) ~~about the impact of no-decay El Niño on rainfall ,~~ showing decreasing Indian summer monsoon rainfall after long-lasting El Niño events, episodes which last until the ~~next winter are selected (~~fall or over the whole year following the El Niño winters are now selected (i.e. the years 1982, 1987 and 1992 ~~) and the~~ listed in Table 1). Here, we investigate whether their mean influence on the atmospheric ~~circulations and ozone distributions was investigated (details are omitted). The SFand~~ circulation and on the ozone distribution, although not statistically significant, will increase the El Niño-related effects derived in the previous sections. Table 2 shows the peak values of SF, VP and Hadley circulation found inside the blue domains in Figures 2, 5 and 6, respectively.

Indeed, SF, VP and Hadley circulation averaged over these three years show strongest anomalies ~~during these two years~~ if compared to all El Niño years. In particular, the ASM anticyclone is ~~even~~ weaker and the Hadley circulation is stronger ~~during these periods~~for most considered months following the long-lasting El Niño winters. The onset date of the ASM after long-lasting El Niños is even slightly later than after the other El Niño winters (Fig. 3). Accordingly, the ozone concentrations in the tropics ~~show weak~~ are less disturbed by isentropic intrusions from the subtropics~~during summer~~. Consequently, lowest ozone concentrations are detected in the blue domain in Figure 10 until the end of summer, at which time ozone following long-lasting El Niños switches to having the highest values in the early fall (cyan line in Figure 10). This indicates that if El Niño does not decay until the following summer, ~~the influence of El Niño~~ its influence on the ASM anticyclone and ozone will last longer.

Neu et al. (2014) found that the superposition of El Niño and easterly QBO phase increases ozone flux from the stratosphere into the troposphere, resulting in enhanced tropospheric ozone values in mid-latitudes. ~~In particular, increased convection over~~

Number of months	La Niña			El Niño			long-lasting El Niño		
after ENSO winter	SF	VP ~~distributions~~	HC	SF	VP	HC	SF	VP	HC
0	34	127	24	25	83	26	25	135	29
1	34	115	21	25	73	22	25	111	24
2	26	112	16	17	55	15	18	78	21
3	26	108	15	6	55	16	8	41	23
4	14	120	17	5	93	21	2	58	29
5	23	147	18	14	131	23	8	82	31
6	29	148	16	27	145	20	23	95	27

Table 2. List of the maximum strength of the NH anticyclone (SF in 10^6 m^2/s), Walker circulation (VP in 10^5 m^2/s) and Hadley circulation (HC in 10^5 m^2/s) after La Niña, El Niño and long-lasting El Niño found inside the blue domains in Figures 2, 5 and 6, respectively.

~~the central/eastern Pacific results in a negative zonal mean ozone anomaly in the tropical upper troposphere.~~ The opposite effect occurs for the combination of La ~~Niñ~~Niña and westerly QBO phase. ~~Here, we also check the influence of QBO on the~~ Motivated by this study, we investigate how the QBO phase affects our results. Table 1 shows that La Niña winters are almost equally affected by westerly and easterly QBO phases, while during El Niño the westerly QBO phase occurs more often. To ~~remove~~ quantify the potential influence of the QBO phase, ~~the results from 4 years of westerly QBO (1997/1998 and 2006/2007) are excluded. The change of ozone concentration~~ we compare the difference between La Niña and El Niño subcomposites defined by the westerly and easterly phases. The CLaMS results in the blue rectangle at 380 K ~~caused by ENSO is around 3% based on CLaMS simulations from winter to summer, the westerly phase causes slightly higher ozone concentration than easterly in the tropical upper troposphere. The change is less than 5% from SHADOZ data, and~~ (Fig. 10 (c)) show that the ozone concentration after La Niña events is higher than after El Niño events during both phases of the QBO, but their difference is larger during the easterly than during the westerly QBO phase. Similarly, the SHADOZ ozone data (Figure 11) shows that the ozone concentration after La Niña events is higher (lower) than after El Niño events in the UTLS (middle troposphere) during both phases of the QBO, while the respective subcomposites show larger differences during the easterly than during the westerly phase~~also causes slightly higher ozone in the UTLS region in Hilo~~. This indicates that our results ~~about~~ on the ENSO effects are robust, but the difference will be enhanced (weakened) during the easterly (westerly) phase of the QBO.

6 Conclusions

ENSO typically shows the strongest signal in boreal winter, but it can affect the ~~atmosphere~~ atmospheric circulation and constituent distributions until the next ~~early summer. Here we try to understand~~ fall. To quantify the influence of ENSO on the ~~UTLS~~ atmosphere from a dynamical ~~and atmospheric composition perspective. SFand VP are introduced to quantify the influence of ENSO on the atmosphere from a dynamical perspective~~perspective, the stream function (SF) and the velocity

potential (VP) are introduced. SF and VP represent the ~~divergence free and rotation free~~ divergence-free and the rotation-free part of the horizontal wind field, respectively. The results show that the subtropical jets after El Niño winters are more zonally symmetric than after La Niña winters. Furthermore, the meridional disruption of the subtropical jets during El Niño ~~is~~ are weaker compared to La Niña winters. The anticyclonic ~~circulations~~ circulation in the tropics following El Niño is weaker than following La Niña. The strength of the ASM anticyclone after El Niño is slightly weaker than after La Niña in early boreal summer, and the onset date ~~after~~ in El Niño years is about half a month later than ~~after~~ in La Niña years. VP after El Niño is weaker than after La Niña from winter until early summer because of the weaker Walker circulation ~~after~~ in El Niño years. The Hadley circulation after El Niño is much stronger than after La Niña from winter to spring.

The anomalies of the atmospheric circulation caused by ENSO also affect the distribution of atmospheric composition. MLS satellite measurements (2004-2015) and CLaMS simulations (1979-2015) are used to analyse the ~~horizontal~~ influence of ENSO on the ozone distribution in the vicinity of the tropopause (380 K). The results from CLaMS simulations show similar patterns as MLS measurements. ~~They bothmanifest that~~ In both, ozone patterns after La Niña winters and springs show in-mixing over the east and central Pacific, while the ozone patterns after El Niño winters and springs are more zonally symmetric. The in-mixing difference between La Niña and El Niño is striking during the onset of the ASM anticyclone ~~. The intrusions~~ (AMJ). Intrusions from the high latitude stratosphere reach much deeper into the tropics ~~for~~ after La Niña ~~compared to~~ winters than after El Niño winters. This indicates that the ozone anomaly lags the atmospheric circulation anomaly in El Niño/La Niña winters by about 4 months. ~~The weaker in-mixing and strong Hadley circulation during El Niño causes smaller ozone mixing ratio in the tropics compared to La Niña in the UTLS from winter to early summer.~~

Based on the ozonesonde data from SHADOZ (1998-2015) in Hilo, Hawaii, the vertical impact of ENSO on the ozone distribution is investigated. The ~~common~~ "well known" vertical "S" shape structure only exists in the ozone profiles following El Niño ~~rather than~~ but not La Niña from winter to early summer. The ozone concentration in the UTLS after El Niño is lower than after La Niña from DJF to AMJ. ~~The~~ Our results demonstrate that the air masses over Hilo following La Niña encounter stronger (weaker) in-mixing ~~comparing~~ in the UTLS (middle troposphere) compared to El Niño. ~~This significantly changes the ozone profiles after~~

Weaker in-mixing and stronger Hadley circulation due to El Niño cause lower ozone mixing ratios in the tropical UTLS compared to La Niña from winter to early summer. However, the in-mixed ozone following El Niño winters may become higher in the subtropical middle troposphere as well as in the TTL in late summer and fall. This effect is related to a stronger Hadley/BD-circulation after El Niño compared to La Niña~~years~~, which may cause higher ozone values in the extratropics and, consequently, stronger isentropic and meridional gradients of ozone after El Niño winters. The duration and intensity of the El Niño related anomalies are amplified if only the long-lasting episodes are considered. The ENSO related anomalies are enhanced (weakened) during the easterly (westerly) phase of the QBO.

~~0.2~~

Acknowledgements. This work was supported by International Postdoctoral Exchange Fellowship Program 2015 under grant No. 20151011. The European Centre for Medium-Range Weather Forecasts (ECMWF) provided meteorological analysis for this study. ~~Ozonesonde date were~~ OLR and ENSO MEI index data is provided by NOAA. Ozonesonde data is provided through the SHADOZ database. Work at the Jet Propulsion Laboratory, California Institute of Technology, was carried out under a contract with the National Aeronautics and Space Administration. We would like to thank Suvarna Fadnavis for some discussions which motivated us to do this work. The stream function and velocity potential are calculated based on the method from H. L. Tanaka. Excellent programming support was provided by N. Thomas.

References

Bannister, R. N., O'Neill, A., Gregory, A. R., and Nissen, K. M.: The role of the south-east Asian monsoon and other seasonal features in creating the 'tape-recorder' signal in the Unified Model, Q. J. R. Meteorol. Soc., 130, 1531–1554, 2004.

Bjerknes, J.: Atmospheric teleconnections from the equatorial Pacific, Monthly Weather Review, 97, 163–172, 1969.

Bjerknes, V.: Sur les relations entre l'ozone et les mouvements de la troposphère, Gerl. Beitr. Geophys., 24, 23, 1929.

Calvo, N., Garcia, R. R., Randel, W. J., and Marsh, D.: Dynamical mechanism for the increase in tropical upwelling in the lowermost tropical stratosphere during warm ENSO events, J. Atmos. Sci., 67, 2331–2340, https://doi.org/10.1175/2010JAS3433.1, 2010.

Chen, P.: Isentropic cross-tropopause mass exchange in the extratropics, J. Geophys. Res., 100, 16 661–16 673, 1995.

Chowdary, J. S., Harsha, H. S., Gnanaseelan, C., Srinivas, G., Parekh, A., Pillai, P., and Naidu, C. V.: Indian summer monsoon rainfall variability in response to differences in the decay phase of El Niño, Climate Dynamics, https://doi.org/10.1007/s00382-016-3233-1, 2016.

Dee, D. P., Uppala, S. M., Simmons, A. J., Berrisford, P., Poli, P., Kobayashi, S., Andrae, U., Balmaseda, M. A., Balsamo, G., Bauer, P., Bechtold, P., Beljaars, A. C. M., van de Berg, L., Bidlot, J., Bormann, N., Delsol, C., Dragani, R., Fuentes, M., Geer, A. J., Haimberger, L., Healy, S. B., Hersbach, H., Holm, E. V., Isaksen, L., Kallberg, P., Koehler, M., Matricardi, M., McNally, A. P., Monge-Sanz, B. M., Morcrette, J.-J., Park, B.-K., Peubey, C., de Rosnay, P., Tavolato, C., Thepaut, J.-N., and Vitart, F.: The ERA-Interim reanalysis: configuration and performance of the data assimilation system, Q. J. R. Meteorol. Soc., 137, 553–597, https://doi.org/10.1002/qj.828, 2011.

Dethof, A., O'Neill, A., Slingo, J. M., and Smit, H. G. J.: A mechanism for moistening the lower stratosphere involving the Asian summer monsoon, Q. J. R. Meteorol. Soc., 556, 1079–1106, 1999.

Dunkerton, T. J.: Evidence of meridional motion in the summer lower stratosphere adjacent to monsoon regions, J. Geophys. Res., 100, 16,675–16,688, 1995.

Evans, J. L. and Allan, R. J.: El Nino/southern oscillation modification to the structure of the monsoon and tropical cyclone activity in the Australasian region, International Journal of Climatology, 12, 611–623, 1992.

Folkins, I., Braun, C., Thompson, A. M., and Witte, J.: Tropical ozone as an indicator of deep convection, Journal of Geophysical Research: Atmospheres, 107, ACH 13–1–ACH 13–10, https://doi.org/10.1029/2001JD001178, http://dx.doi.org/10.1029/2001JD001178, 2002.

Fu, R., Hu, Y., Wright, J. S., Jiang, J. H., Dickinson, R. E., Chen, M., Filipiak, M., Read, W. G., Waters, J. W., and Wu, D. L.: Short circuit of water vapor and polluted air to the global stratosphere by convective transport over Tibetian Plateau, Proc. Nat. Acad. Sci., 103, 5664–5669, 2006.

Fueglistaler, S., Bonazzola, M., Haynes, P. H., and Peter, T.: Stratospheric water vapor predicted from the Lagrangian temperature history of air entering the stratosphere in the tropics, J. Geophys. Res., 110, D08107, https://doi.org/10.1029/2004JD005516, 2005.

Garfinkel, C. I., Hurwitz Margaret, M., Oman Luke, D., and Waugh, D. W.: Contrasting Effects of Central Pacific and Eastern Pacific El Nino on stratospheric water vapor, grl, 40, 4115–4120, https://doi.org/10.1002/grl.50677, 2013.

Gettelman, A., Hoor, P., Pan, L. L., Randel, W. J., Hegglin, M. I., and Birner, T.: The extratropical upper troposphere and lower stratosphere, Rev. Geophys., 49, RG3003, https://doi.org/10.1029/2011RG000355, 2011.

Gill, A. E.: Some simple solutions for heat-induced tropical circulation, Q. J. R. Meteorol. Soc., 106, 447–462, 1980.

Hayashi, H., Kita, K., and Taguchi, S.: Ozone-enhanced layers in the troposphere over the equatorial Pacific Ocean and the influence of transport of midlatitude UT/LS air, Atmos. Chem. Phys., 8, 2609–2621, 2008.

Haynes, P. and Shuckburgh, E.: Effective diffusivity as a diagnostic of atmospheric transport, 2, Troposphere and lower stratosphere, J. Geophys. Res., 105, 22 795–22 810, 2000.

Highwood, E. J. and Hoskins, B. J.: The tropical tropopause, Q. J. R. Meteorol. Soc., 124, 1579 – 1604, 1998.

Holton, J. R., Haynes, P., McIntyre, M. E., Douglass, A. R., Rood, R. B., and Pfister, L.: Stratosphere-troposphere exchange, Rev. Geophys., 33, 403–439, 1995.

Jiang, Y. B., Froidevaux, L., Lambert, A., Livesey, N. J., Read, W. G., Waters, J. W., Bojkov, B., Leblanc, T., McDermid, I. S., Godin-Beekmann, S., Filipiak, M. J., Harwood, R. S., Fuller, R. A. , Daffer, W. H., Drouin, B. J., Cofield, R. E., Cuddy, D. T., Jarnot, R. F., Knosp, B. W., Perun, V. S., Schwartz, M. J., Snyder, W. V., Stek, P. C., Thurstans, R. P., Wagner, P.

Hope, A. C. A., Allaart, M., Andersen, S. B., Bodeker, G., Calpini, B., Claude, H., Coetzee, G., Davies, J., De Backer, H., Dier, H., Fujiwara, M., Johnson, B., Kelder, H., Leme, N. P., König-Langlo, G., Kyro, E., Laneve, G., Fook, L. S., Merrill, J., Morris, G., Newchurch, M., Oltmans, S., Parrondos, M. C., Posny, F., Schmidlin, F., Skrivankova, P., Stubi, R., Tarasick, D., Thompson, A ., Thouret, V., Viatte, P., V: öA Simplified Monte Carlo Significance Test Procedure mel, H., von Der Gathen, P., Yela, M. , and Zablocki, G.: Validation of Aura Microwave Limb Sounder Ozone by ozonesonde and lidar measurements, Journal of Geophysical Research: Atmospheres, 112, 2007. Journal of the Royal Statistical Society. Series B (Methodological), 30, 582–598, http://www.jstor.org/stable/2984263, 1968.

Ju, J. and Slingo, J.: The Asian summer monsoon and ENSO, Quarterly Journal of the Royal Meteorological Society, 121, 1133–1168, 1995.

Kawamura, R.: A Possible Mechanism of the Asian Summer Monsoon-ENSO Coupling, Journal of the Meteorological Society of Japan. Ser. II, 76, 1009–1027, 1998.

Konopka, P. and Pan, L. L.: On the mixing-driven formation of the Extratropical Transition Layer (ExTL), J. Geophys. Res., 117, D18301, , 2012.

Konopka, P., Steinhorst, H.-M., Grooß, J.-U., Günther, G., Müller, R., Elkins, J. W., Jost, H.-J., Richard, E., Schmidt, U., Toon, G., and McKenna, D. S.: Mixing and Ozone Loss in the 1999-2000 Arctic Vortex: Simulations with the 3-dimensional Chemical Lagrangian Model of the Stratosphere (CLaMS), J. Geophys. Res., 109, D02315, https://doi.org/10.1029/2003JD003792, 2004.

Konopka, P., Grooß, J.-U., Günther, G., Ploeger, F., Pommrich, R., Müller, R., and Livesey, N.: Annual cycle of ozone at and above the tropical tropopause: observations versus simulations with the Chemical Lagrangian Model of the Stratosphere (CLaMS), Atmos. Chem. Phys., 10, 121–132, https://doi.org/10.5194/acp-10-121-2010, http://www.atmos-chem-phys.net/10/121/2010/, 2010.

Konopka, P., Ploeger, F., Tao, M., and Riese, M.: Zonally resolved impact of ENSO on the stratospheric circulation and water vapor entry values, Journal of Geophysical Research: Atmospheres, 121, 11,486–11,501, 2016.

Krüger, K., Tegtmeier, S., and Rex, M.: Long-term climatology of air mass transport through the Tropical Tropopause Layer (TTL) during NH winter, Atmos. Chem. Phys., 8, 813–823, 2008.

Kunze, M., Braesicke, P., Langematz, U., and Stiller, G.: Interannual variability of the boreal summer tropical UTLS in observations and CCMVal-2 simulations, Atmospheric Chemistry and Physics, 16, 8695–8714, https://doi.org/10.5194/acp-16-8695-2016, https://www.atmos-chem-phys.net/16/8695/2016, 2016.

Liess, S. and Geller, M. A.: On the relationship between QBO and distribution of tropical deep convection, J. Geophys. Res., 117, D03108, https://doi.org/10.1029/2011JD016317, 2012.

Livesey, N. J., Read, W. G., Wagner, P. A., Froidevaux, L., Lambert, A., Manney, G. L., Valle, L. F. M., Pumphrey, H. C., Santee, M. L., Schwartz, M. J., Wang, S., Fuller, R. A., Jarnot, R. F., Knosp, B. W., and Martinez, E.: Version 4.2x Level 2 data quality and description document, 2017.

Matsuno, T.: Quasi-geostrophic motopns in the equatorial area, J. Meteorol. Soc. Jpn., 44, 25–42, 1966.

McKenna, D. S., Konopka, P., Grooß, J.-U., Günther, G., Müller, R., Spang, R., Offermann, D., and Orsolini, Y.: A new Chemical Lagrangian Model of the Stratosphere (CLaMS): 1. Formulation of advection and mixing, J. Geophys. Res., 107, 4309, https://doi.org/10.1029/2000JD000114, 2002.

McPhaden, M. J.: Playing hide and seek with El Nino, Nature Climate Change, 5, 791–795, 2015.

McPhaden, M. J., Zebiak, S. E., and Glantz, M. H.: ENSO as an integrating concept in Earth science, Science, 314, 1740–1745, 2006.

Moron, V. and Gouirand, I.: Seasonal modulation of the El Niño–southern oscillation relationship with sea level pressure anomalies over the North Atlantic in October–March 1873–1996, International Journal of Climatology, 23, 143–155, https://doi.org/10.1002/joc.868, http://dx.doi.org/10.1002/joc.868, 2003.

Müller, S., Hoor, P., Bozem, H., Gute, E., Vogel, B., Zahn, A., Bönisch, H., Keber, T., Krämer, M., Rolf, C., Riese, M., Schlager, H., and Engel, A.: Impact of the Asian monsoon on the extratropical lower stratosphere: trace gas observations during TACTS over Europe 2012, Atmospheric Chemistry & Physics, 16, 10 573–10 589, https://doi.org/10.5194/acp-16-10573-2016, 2016.

Neu, J. L., Flury, T., Manney, G. L., Santee, M. L., Livesey, N. J., and Worden, J.: Tropospheric ozone variations governed by changes in stratospheric circulation, Nature Geosci, 7, 340–344, https://doi.org/10.1038/ngeo2138, 2014.

~~Pan, L. L., Konopka~~

Newell, R. E., Thouret, V., Cho, J. Y. N., Stoller, P., ~~and Browell, E. V~~Marenco, A., and Smit, H. G.: ~~Observations and model simulations of mixing near the extratropical tropopause~~Ubiquity of quasi-horizontal layers in the troposphere, ~~J. Geophys.Res.~~Nature, 398, 316 – 319, 1999.

Pan, L. L., Honomichl, S. B., Randel, W. J., Apel, E. C., Atlas, E. L., Beaton, S. P., Bresch, J. F., Hornbrook, R., Kinnison, D. E., Lamarque, J. F., Saiz-Lopez, A., Salawitch, R. J., and Weinheimer, A. J.: Bimodal distribution of free tropospheric ozone over the tropical western Pacific revealed by airborne observations , ~~111, D05106, , 2006.~~ Geophysical Research Letters, 42, 7844–7851, 2015.

Park, M., Randel, W. J., Gettelman, A., Massie, S. T., and Jiang, J. H.: Transport above the Asian summer monsoon anticyclone inferred from Aura Microwave Limb Sounder tracers, Journal of Geophysical Research: Atmospheres, 112, 2007.

Park, M., Randel, W. J., Emmons, L. K., Bernath, P. F., Walker, K. A., and Boone, C. D.: Chemical isolation in the Asian monsoon anticyclone observed in Atmospheric Chemistry Experiment (ACE-FTS) data, Atmos. Chem. Phys., 8, 757–764, 2008.

Philander, S., Holton, J., and Dmowska, R.: El Nino, La Nina, and the Southern Oscillation, vol. 46 of International Geophysics, Academic Press, ~~,~~1989.

Ploeger, F., Konopka, P., Müller, R., Fueglistaler, S., Schmidt, T., Manners, J. C., Grooß, J.-U., Günther, G., Forster, P. M., and Riese, M.: Horizontal transport affecting trace gas seasonality in the Tropical Tropopause Layer (TTL), J. Geophys. Res., 117, D09303, https://doi.org/10.1029/2011JD017267, ~~warning: BibtexKey has changed!!,~~ 2012.

Ploeger, F., Günther, G., Konopka, P., Fueglistaler, S., Müller, R., Hoppe, C., Kunz, A., Spang, R., Grooß, J.-U., and Riese, M.: Horizontal water vapor transport in the lower stratosphere from subtropics to high latitudes during boreal summer, J. Geophys. Res., 118, 8111–8127, https://doi.org/10.1002/jgrd.50636, 2013.

Ploeger, F., Riese, M., Haenel, F., P.Konopka, Müller, R., and Stiller, G.: Variability of stratospheric mean age of air and of the local effects of residual circulation and eddy mixing, J. Geophys. Res., 120, 716–733, https://doi.org/10.1002/2014JD022468, 2015.

Ploeger, F., Konopka, P., Walker, K., and Riese, M.: Quantifying pollution transport from the Asian monsoon anticyclone into the lower stratosphere, Atmos. Chem. Phys., 16, 7055–7066, https://doi.org/10.5194/acp-17-7055-2017, 2017.

Pommrich, R., Müller, R., Grooß, J.-U., Konopka, P., Ploeger, F., Vogel, B., Tao, M., Hoppe, C. M., Günther, G., Spelten, N., Hoffmann, L., Pumphrey, H.-C., Viciani, S., D'Amato, F., Volk, C. M., Hoor, P., Schlager, H., and Riese, M.: Tropical troposphere to stratosphere

transport of carbon monoxide and long-lived trace species in the Chemical Lagrangian Model of the Stratosphere (CLaMS), Geoscientific Model Development, 7, 2895–2916, https://doi.org/10.5194/gmd-7-2895-2014, http://www.geosci-model-dev.net/7/2895/2014/, 2014.

Pumphrey, H. C., Glatthor, N., Bernath, P. F., Boone, C. D., Hannigan, J., Ortega, I., Livesey, N. J., and Read, W. G.: MLS measurements of stratospheric hydrogen cyanide during the 2015–16 El Niño event, Atmospheric Chemistry and Physics Discussions, 2017, 1–18, 2017.

Randel, W. J. and Park, M.: Deep convective influence on the Asian summer monsoon anticyclone and associated tracer variability observed with Atmospheric Infrared Sounder (AIRS), J. Geophys. Res., 111, D12314, https://doi.org/10.1029/2005JD006490, 2006.

Randel, W. J., Garcia, R. R., Calvo, N., and Marsh, D.: ENSO influence on zonal mean temperature and ozone in the tropical lower stratosphere, Geophys. Res. Lett., 36, L15822, https://doi.org/10.1029/2009GL039343, 2009.

Randel, W. J., Park, M., Emmons, L., Kinnison, D., Bernath, P., Walker, K. A., Boone, C., and Pumphrey, H.: Asian Monsoon Transport of Pollution to the Stratosphere, Science, 328, 611–613, https://doi.org/10.1126/science.1182274, 2010.

Rolf, C., Vogel, B., Hoor, P., Afchine, A., Günther, G., Krämer, M., Müller, R., Müller, S., Spelten, N., and Riese, M.: Water vapor increase in the ~~northern lower stratosphere by~~ lower stratosphere of the Northern Hemisphere due to the Asian monsoon anticyclone observed during the TACTS/ESMVal campaigns, Atmospheric Chemistry and Physics~~Discussions, 2017, 1–16, 2017.~~, 18, 2973–2983, 2018.

Roxy, M. K., Ritika, K., Terray, P., Murtugudde, R., Ashok, K., and Goswami, B. N.: Drying of Indian subcontinent by rapid Indian Ocean warming and a weakening land-sea thermal gradient, Nature Communications, 6, 2015.

Santee, M. L., Manney, G. L., Livesey, N. J., Froidevaux, L., Schwartz, M. J., and Read, W. G.: Trace gas evolution in the lowermost stratosphere from Aura Microwave Limb Sounder measurements, J. Geophys. Res., 116, 2011.

Santee, M. L., Manney, G. L., Livesey, N. J., Schwartz, M. J., Neu, J., and Read, W. G.: A comprehensive overview of the climatological composition of the Asian summer monsoon anticyclone based on 10 years of Aura Microwave Limb Sounder measurements, J. Geophys. Res., 122, 2017.

Scaife, A. A., Butchart, N., Jackson, D. R., and Swinbank, R.: Can changes in ENSO activity help to explain increasing stratospheric water vapor?, Geophys. Res. Lett., 30, https://doi.org/10.1029/2003GL017591, 2003.

Tanaka, H. L., Ishizaki, N., and Kitoh, A.: Trend and interannual variability of Walker, monsoon and Hadley circulations defined by velocity potential in the upper troposphere, Tellus A, 56, 250–269, 2004.

Thompson, A. M., Witte, J. C., Smit, H. G. J., Oltmans, S. J., Johnson, B. J., Kirchhoff, V. W. J. H., and Schmidlin, F. J.: Southern Hemisphere Additional Ozonesondes (SHADOZ) 1998-2004 tropical ozone climatology: 3. Instrumentation, station-to-station variability, and evaluation with simulated flight profiles, J. Geophys. Res., 112, 1297–1300, https://doi.org/10.1029/2005JD007042, 2007.

Thompson, A. M., Miller, S. K., Tilmes, S., Kollonige, D. W., Witte, J. C., Oltmans, S. J., Johnson, B. J., Fujiwara, M., Schmidlin, F. J., Coetzee, G. J. R., Komala, N., Maata, M., bt Mohamad, M., Nguyo, J., Mutai, C., Ogino, S.-Y., Da Silva, F. R., Leme, N. M. P., Posny, F., Scheele, R., Selkirk, H. B., Shiotani, M., Stübi, R., Levrat, G., Calpini, B., Thouret, V., Tsuruta, H., Canossa, J. V., Vömel, H., Yonemura, S., Diaz, J. A., Tan Thanh, N. T., and Thuy Ha, H. T.: Southern Hemisphere Additional Ozonesondes (SHADOZ) ozone climatology (2005–2009): Tropospheric and tropical tropopause layer (TTL) profiles with comparisons to OMI-based ozone products, Journal of Geophysical Research: Atmospheres, 117, 2012.

Thouret, V., Cho, J. Y. N., Evans, M. J., Newell, R. E., Avery, M. A., Barrick, J. D. W., Sachse, G. W., and Gregory, G. L.: Tropospheric ozone layers observed during PEM-Tropics B, J. Geophys. Res., 106, 32 527–32 538, 2001.

Thouret, V., Cammas, J.-P., Sauvage, B., Athier, G., Zbinden, R., Nédélec, P., Simon, P., and Karcher, F.: Tropopause referenced ozone climatology and inter-annual variability (1994–2003) from the MOZAIC programme, Atmospheric Chemistry and Physics, 6, 1033–1051, 2006.

Vogel, B., Günther, G., Müller, R., Grooß, J.-U., Afchine, A., Bozem, H., Hoor, P., Krämer, M., Müller, S., Riese, M., Rolf, C., Spelten, N., Stiller, G. P., Ungermann, J., and Zahn, A.: Long-range transport pathways of tropospheric source gases originating in Asia into the northern lower stratosphere during the Asian monsoon season 2012, Atmospheric Chemistry and Physics, 16, 15 301–15 325, 2016.

Walker, G. T.: Correlation in seasonal variations of weather. VIII: A preliminary study of world weather, 1923.

Wang, C. and Picaut, J.: Understanding ENSO physics - A review, in: Earth's Climate: The Ocean-Atmosphere Interaction, edited by Wang, C., Xie, S.-P., and Carton, J. A., vol. 147 of Geophysical Monograph Series, pp. 21–38, AGU, 2004.

Wang, H. J., Cunnold, D. M., Thomason, L. W., Zawodny, J. M., and Bodeker, G. E.: Assessment of SAGE version 6.1 ozone data quality, J. Geophys. Res., 105, 4691, https://doi.org/10.1029/2002JD002418, 2002.

Wang, X., Jiang, X., Yang, S., and Li, Y.: Different impacts of the two types of El Niño on Asian summer monsoon onset, Environmental Research Letters, 8, 044 053, http://stacks.iop.org/1748-9326/8/i=4/a=044053, 2013.

Waugh, D. W. and Polvani, L. M.: Climatology of intrusions into the tropical upper troposphere, Geophys. Res. Lett., 27, 3857–3860, 2000.

Wolter, K.: The Southern Oscillation in surface circulation and climate over the tropical Atlantic, Eastern Pacific, and Indian Oceans as captured by cluster analysis., J. Climate Appl. Meteor., 26, 540–558, 1987.

Wolter, K. and Timlin, M. S.: El Niño/Southern Oscillation behaviour since 1871 as diagnosed in an extended multivariate ENSO index (MEI.ext), International Journal of Climatology, 31, 1074–1087, https://doi.org/10.1002/joc.2336, 2011.

Wright, J. S., Fu, R., Fueglistaler, S., Liu, Y. S., and Zhang, Y.: The influence of summertime convection over Southeast Asia on water vapor in the tropical stratosphere, J. Geophys. Res., 116, D12302, https://doi.org/10.1029/2010JD015416, 2011.

Yan, X., Wright, J. S., Zheng, X., Livesey, N. J., Vömel, H., and Zhou, X.: Validation of Aura MLS retrievals of temperature, water vapour and ozone in the upper troposphere and lower–middle stratosphere over the Tibetan Plateau during boreal summer, Atmospheric Measurement Techniques, 9, 3547–3566, https://doi.org/10.5194/amt-9-3547-2016, https://www.atmos-meas-tech.net/9/3547/2016/, 2016.

Zhang, Z. and Krishnamurti, T. N.: A Generalization of Gill's Heat-Induced Tropical Circulation, J. Atmos. Sci., 53, 1045–1052, 2006.

Ziemke, J. R., Douglass, A. R., Oman, L. D., Strahan, S. E., and Duncan, B. N.: Tropospheric ozone variability in the tropics from ENSO to MJO and shorter timescales, Atmospheric Chemistry and Physics, 15, 8037–8049, 2015.